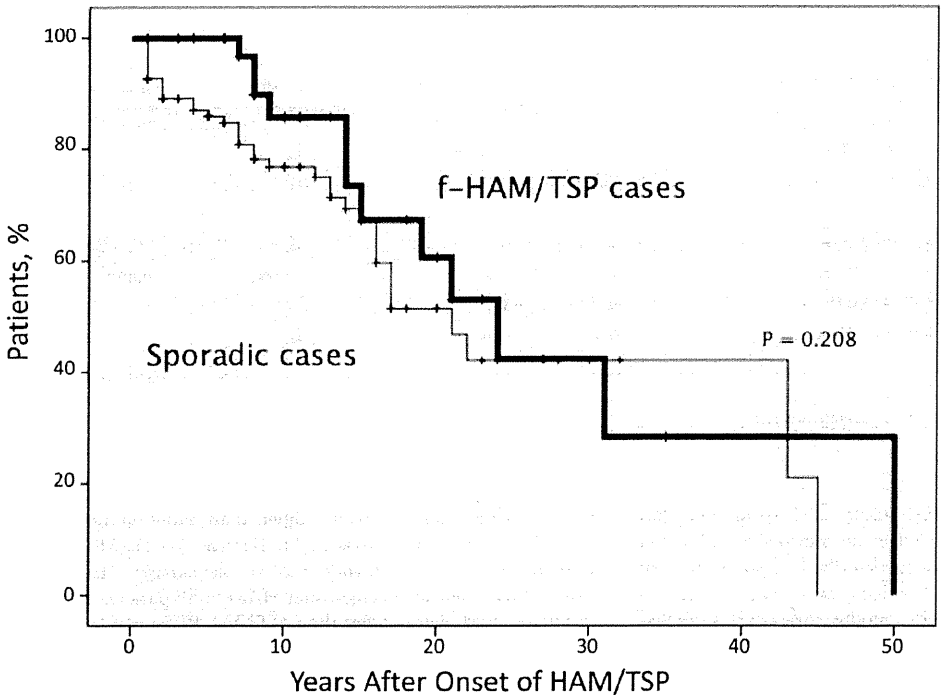

Figure 1. Kaplan–Meier estimates of the time from disease onset to assignment of motor disability scores of 6. In sporadic cases, more patients reached the score of six at an early stage; however, the difference was not significant. Approximately 30% of both f-HAM/TSP cases and sporadic cases needed a wheelchair in daily life in 15 years after onset and approximately 50% of patients from both groups needed a wheelchair in 20 years after onset.
doi:10.1371/journal.pone.0086144.g001

than in male. There was no significant difference between women and men in the age of onset (61.5 y.o.±12.6 vs. 62.7 y.o.±12.5), in the incidence of rapid progression (26.3% vs. 32.3%) and in MDG score (5.4 vs. 5.0; mean).

Discussion

We demonstrated that among 784 HAM/TSP patients, 40 (5.1%) had family members with the disease. The lifetime risk of developing HAM/TSP is 0.25% of HTLV-1 carriers in Japan

Table 1. Clinical features of f-HAM/TSP cases or sporadic cases of HAM/TSP.

	f-HAM/TSP cases (40 cases)	Sporadic cases (124 cases)	p value	p value*
Female ratio (%)	78.8% (7 males : 33 females)	66.4% (31 males : 93 females)	NS	
Age	55.6±13.0 (23–79)	61.8±12.5 (15–83)	**0.008**	
Age of onset	41.3±13.9 (14–65)	51.6±15.9 (13–78)	**<0.001**	**0.017**
Duration of illness (years)	14.3±11.4 (1–49)	10.2±9.6 (0–45)	**0.026**	**0.017**
Initial symptoms				
Gait disturbance	50.0%	52.4%	NS	
Urinary disturbance	32.5%	26.6%	NS	
Sensory disturbance	12.5%	14.5%	NS	
Others	5%	6.5%	NS	
Rapid disease progression	4 cases (10.0%)	35 cases (28.2%)	**0.019**	0.069
Motor disability score	4.0±2.0 (0–7)	4.9±1.5 (0–8)	**0.043**	**0.036**
Score more than 6	12 cases (30.0%)	38 cases (30.7%)	NS	
Time elapsed between onset and wheelchair use in daily life (years)	18.3±12.4 (7–50)	10.0±10.4 (1–45)	**0.025**	**0.020**

Data are presented as mean values ± s.d., (range),
*Adjusted for age and sex.
doi:10.1371/journal.pone.0086144.t001

Table 2. Laboratory findings of familial clusters or sporadic cases of HAM/TSP.

	f-HAM/TSP cases (40cases)	Sporadic cases (124 cases)	p value	p value†
Anti-HTLV-1 antibodies*				
Titer in Serum	20,787±31,004, N=37	31,009±36,075, N=109	NS	
Titer in CSF	2,310±11,741, N=31	672±1,274, N=111	NS	
Cerebrospinal fluid				
Cell number (/mm^3)	3.0±2.5, N=25	5.7±10.0, N=109	NS	
Protein (mg/dl)	29.9±9.4, N=22	42.5±19.3, N=109	**<0.001**	**0.007**
Neopterin (pmol/ml)	83.2±118.1, N=18	38.3±56.8, N=35	NS	
HTLV-1 proviral loads (Copies/10^4 PBMCs)	930±781, N=32	968±1,746, N=101	NS	

* Particle Aggregation Method.
Data are presented as mean values ± s.d., N=sample number,
†Adjusted for age and sex.
doi:10.1371/journal.pone.0086144.t002

[13]. Although clustering of familial adult T-cell lymphomas has been reported [8,9], to our knowledge the prevalence of familial clusters of HAM/TSP has not been described. A study in Peru showed that 30% of HAM/TSP patients have family members with paralytic neurological disorders, but the cause of paralysis was not evaluated [14]. In the present study, we included f-HAM/TSP diagnosed in medical institutions and excluded cases with a family history of neurological disorders. Thus, the actual incidence rates of f-HAM/TSP may be higher than those reported here. Interestingly, although HTLV-1 PVL has been associated with the development and clinical progression of HAM/TSP [15–17], there was no significant difference between f-HAM/TSP and sporadic cases in the present study. Because previous studies reported that HTLV-1 PVLs of asymptomatic carriers in relatives of HAM/TSP patients were higher than those in non-HAM-related asymptomatic carriers [6], relatives of HAM/TSP are believed to be at a higher risk of developing HAM/TSP. Interestingly, our data suggest that HAM/TSP patients aggregate in families and factors other than HTLV-1 PVLs may contribute to HAM/TSP.

Compared with sporadic HAM/TSP, the clinical characteristics of f-HAM/TSP have a younger age of onset and longer time elapsed between onset and wheelchair use in daily life. Although we were unable to identify the reason for earlier onset among f-HAM/TSP cases, one can speculate that mild symptoms, such as urinary and sensory disturbances, may be identified earlier by family members who are familiar with HAM/TSP symptoms. However, the present data show no difference in initial symptoms

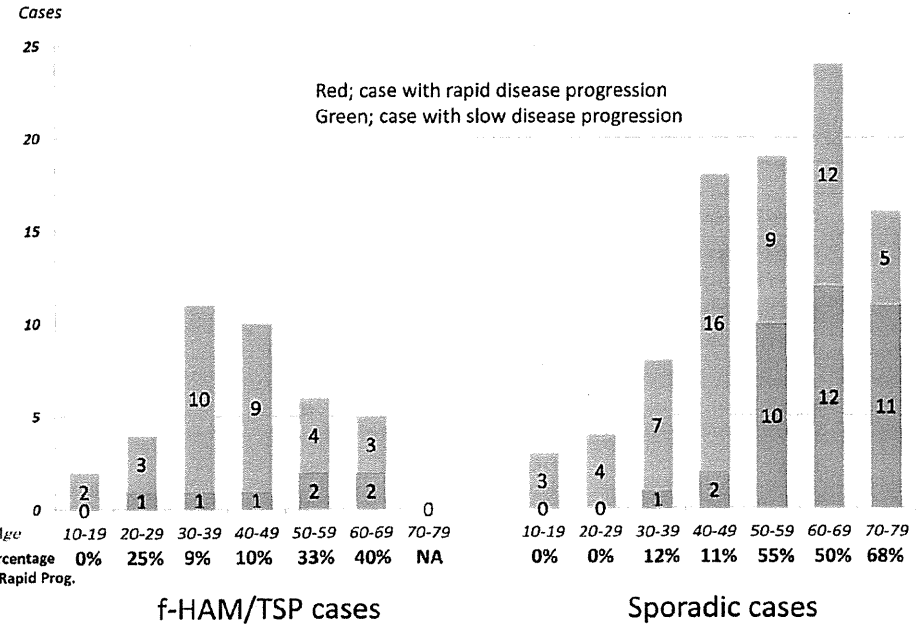

Figure 2. Age-specific proportions of rapid disease progression. The proportion of cases with rapid disease progression tended to increase with the older age of onset.
doi:10.1371/journal.pone.0086144.g002

Table 3. Clinical and laboratory findings of sporadic HAM/TSP with rapid/slow disease progression.

Type of disease progression	Rapid progression	Slow progression	p value
Female ratio (%)	71.4% (10 males : 25 females)	76.4% (21 males : 68 females)	NS
Age of onset	62.3±9.6, N=35	47.4±15.9, N=89	**<0.001**
Age of onset of f-HAM/TSP cases	60.5±3.7, N=4	39.2±12.9, N=36	**0.002**
Duration between onset and inability to walk alone (years)	1.5±0.9, N=13	14.4±10.4, N=25	**<0.001**
Anti-HTLV-1 antibodies*			
Titer in Serum	31,894±36,845, N=34	30,608±35,965, N=75	NS
Titer in CSF	1,251±1,800, N=34	416±852, N=77	**0.014**
Cerebrospinal fluid			
Cell number (/mm^3)	11.6±16.6, N=34	3.2±3.5, N=75	**<0.001**
Protein (mg/dl)	55.3±24.3, N=34	36.7±13.0, N=75	**<0.001**
Neopterin (pmol/ml)	74.9±107.9, N=8	27.4±23.4, N=27	0.255
HTLV-1 proviral loads (Copies/10^4 PBMCs)	370±327, N=32	1,245±2,046, N=69	**<0.001**

* Particle Aggregation Method.
Data are presented as mean values ± s.d., N=sample number.
doi:10.1371/journal.pone.0086144.t003

between f-HAM/TSP and sporadic cases. In all cases, the age of onset and initial symptoms of HAM/TSP were evaluated by the neurologists during hospitalization. Because inflammatory processes are less marked in f-HAM/TSP cases, as indicated by significantly lower protein levels in CSF, f-HAM/TSP cases may show slow progression of disease.

We need to discuss the possibility that the two groups compared represent different mode of HTLV transmission, i.e. vertical vs. sexual transmission. To clarify genetic backgrounds, sporadic HAM/TSP with seropositive carrier family members may be a more appropriate control, but are not available at present. The incidence of female cases showing no significant differences between f-HAM/TSP and sporadic cases, and between rapid and slow disease progression, might suggest less possibility of sporadic cases due to sexual transmission.

Although the subgroup of patients with rapid progression has not been clearly defined, previous studies suggest that rapid progression occurs in 10%–30% of all patients with HAM/TSP [12,14,16], and is associated with an older age of onset [14–16]. In the present study, the age of onset in patients with rapid progression was significantly older than that in patients with slow progression between f-HAM/TSP and sporadic cases, and the proportion of patients with rapid progression increased with the older age of onset (Figure 2). Among sporadic cases, cell numbers and protein levels in CSF were significantly higher in patients with rapid progression, suggesting that inflammation is more active in the spinal cords of patients with rapid progression and that cytotoxic T-lymphocyte (CTL) immune responses may be more intensive. Therefore, lower PVLs in PBMCs of patients with rapid disease progression may be attributed to the strong killing ability of the CTL. However, PVLs were higher in PBMCs of patients with HAM/TSP than in asymptomatic carriers [6]. In addition, the killing ability of CTLs in patients with HAM/TSP does not differ from that in asymptomatic carriers [18]. Hence, strong immune responses may be associated with the disease course. The onset of disease may require other factors that lead to strong immune responses. A late onset may also be associated with alterations of the immune function in HTLV-1-infected patients. Indeed, an increased age has been associated with autoimmune disorders, such as myasthenia gravis and rheumatoid arthritis, and may be partly explained by immune intolerance and accumulation of autoantibodies in older individuals [19,20].

In conclusion, we demonstrated that patients with HAM/TSP aggregate in some families. Compared with sporadic cases, the age of onset was younger and rates of disease progression were slower among familial cases, whereas HTLV-1 PVLs did not differ between f-HAM/TSP and sporadic groups. The present data suggest that factors other than HTLV-1 PVLs contribute to the disease course of HAM/TSP. Our data also suggested strong immune responses in the spinal cord of HAM/TSP patients with rapid progression. Further studies on HTLV-1, immune response to HTLV-1 and genetic factor in patients with rapid progression might provide new insights into HAM/TSP pathogenesis.

Acknowledgments

We would like to express the deepest appreciation to Yuka Komai for collecting information from patients and Dr. Moe Moe Aye for reading our manuscript.

Author Contributions

Conceived and designed the experiments: HT SI OW. Performed the experiments: SN EM. Analyzed the data: SN EM. Contributed reagents/materials/analysis tools: SN EM TM RK. Wrote the paper: SN EM.

References

1. Gessain A, Barin F, Vernant JC, Gout O, Maurs L, et al. (1985) Antibodies to human T-lymphotropic virus type-I in patients with tropical spastic paraparesis. Lancet 2: 407–410.
2. Osame M, Usuku K, Izumo S, Ijichi N, Amitani H, et al. (1986) HTLV-I associated myelopathy, a new clinical entity. Lancet 1: 1031–1032.
3. Proietti FA, Carneiro-Proietti AB, Catalan-Soares BC, Murphy EL (2005) Global epidemiology of HTLV-I infection and associated diseases. Oncogene 24: 6058–6068.
4. Hinuma Y, Nagata K, Hanaoka M, Nakai M, Matsumoto T, et al. (1981) Adult T-cell leukemia: antigen in an ATL cell line and detection of antibodies to the antigen in human sera. Proc Natl Acad Sci U S A 78: 6476–6480.

5. Uchiyama T, Yodoi J, Sagawa K, Takatsuki K, Uchino H (1977) Adult T-cell leukemia: clinical and hematologic features of 16 cases. Blood 50: 481–492.
6. Nagai M, Usuku K, Matsumoto W, Kodama D, Takenouchi N, et al. (1998) Analysis of HTLV-I proviral load in 202 HAM/TSP patients and 243 asymptomatic HTLV-I carriers: high proviral load strongly predisposes to HAM/TSP. J Neurovirol 4: 586–593.
7. Saito M (2010) Immunogenetics and the Pathological Mechanisms of Human T-Cell Leukemia VirusType 1- (HTLV-1-)Associated Myelopathy/Tropical Spastic Paraparesis (HAM/TSP). Interdiscip Perspect Infect Dis 2010: 478461.
8. Pombo-de-Oliveira MS, Carvalho SM, Borducchi D, Dobbin J, Salvador J, et al. (2001) Adult T-cell leukemia/lymphoma and cluster of HTLV-I associated diseases in Brazilian settings. Leuk Lymphoma 42: 135–144.
9. Miyamoto Y, Yamaguchi K, Nishimura H, Takatsuki K, Motoori T, et al. (1985) Familial adult T-cell leukemia. Cancer 55: 181–185.
10. Mori M, Ban N, Kinoshita K (1988) Familial occurrence of HTLV-I–associated myelopathy. Ann Neurol 23: 100.
11. De Castro-Costa CM, Araujo AQ, Barreto MM, Takayanagui OM, Sohler MP, et al. (2006) Proposal for diagnostic criteria of tropical spastic paraparesis/ HTLV-I-associated myelopathy (TSP/HAM). AIDS Res Hum Retroviruses 22: 931–935.
12. Nakagawa M, Izumo S, Ijichi S, Kubota H, Arimura K, et al. (1995) HTLV-I-associated myelopathy: analysis of 213 patients based on clinical features and laboratory findings. J Neurovirol 1: 50–61.
13. Kaplan JE, Osame M, Kubota H, Igata A, Nishitani H, et al. (1990) The risk of development of HTLV-I-associated myelopathy/tropical spastic paraparesis among persons infected with HTLV-I. J Acquir Immune Defic Syndr 3: 1096–1101.
14. Gotuzzo E, Cabrera J, Deza L, Verdonck K, Vandamme AM, et al. (2004) Clinical characteristics of patients in Peru with human T cell lymphotropic virus type 1-associated tropical spastic paraparesis. Clin Infect Dis 39: 939–944.
15. Matsuzaki T, Nakagawa M, Nagai M, Usuku K, Higuchi I, et al. (2001) HTLV-I proviral load correlates with progression of motor disability in HAM/TSP: analysis of 239 HAM/TSP patients including 64 patients followed up for 10 years. J Neurovirol 7: 228–234.
16. Olindo S, Cabre P, Lezin A, Merle H, Saint-Vil M, et al. (2006) Natural history of human T-lymphotropic virus 1-associated myelopathy: a 14-year follow-up study. Arch Neurol 63: 1560–1566.
17. Takenouchi N, Yamano Y, Usuku K, Osame M, Izumo S (2003) Usefulness of proviral load measurement for monitoring of disease activity in individual patients with human T-lymphotropic virus type I-associated myelopathy/ tropical spastic paraparesis. J Neurovirol 9: 29–35.
18. Asquith B, Mosley AJ, Barfield A, Marshall SE, Heaps A, et al. (2005) A functional CD8+ cell assay reveals individual variation in CD8+ cell antiviral efficacy and explains differences in human T-lymphotropic virus type 1 proviral load. J Gen Virol 86: 1515–1523.
19. Manoussakis MN, Tzioufas AG, Silis MP, Pange PJ, Goudevenos J, et al. (1987) High prevalence of anti-cardiolipin and other autoantibodies in a healthy elderly population. Clin Exp Immunol 69: 557–565.
20. Aprahamian T, Takemura Y, Goukassian D, Walsh K (2008) Ageing is associated with diminished apoptotic cell clearance in vivo. Clin Exp Immunol 152: 448–455.

Neurobiology of Disease

Identification and Characterization of $GABA_A$ Receptor Autoantibodies in Autoimmune Encephalitis

Toshika Ohkawa,[1,3] Shin'Ichiro Satake,[2,3] Norihiko Yokoi,[1,3] Yu Miyazaki,[4] Tomohiko Ohshita,[5] Gen Sobue,[4] Hiroshi Takashima,[6] Osamu Watanabe,[6] Yuko Fukata,[1,3]* and Masaki Fukata[1,3]*

[1]Division of Membrane Physiology, Department of Cell Physiology, and [2]Division of Neural Signaling, Department of Information Physiology, National Institute for Physiological Sciences, National Institutes of Natural Sciences; and [3]Department of Physiological Sciences, School of Life Science, The Graduate University for Advanced Studies (SOKENDAI), Okazaki 444-8787, Japan; [4]Department of Neurology, Nagoya University Graduate School of Medicine, Nagoya 466-8550, Japan; [5]Department of Neurology, Suiseikai Kajikawa Hospital, Hiroshima 730-0046, Japan; and [6]Department of Neurology and Geriatrics, Kagoshima University Graduate School of Medical and Dental Sciences, Kagoshima 890-8544, Japan

Autoimmune forms of encephalitis have been associated with autoantibodies against synaptic cell surface antigens such as NMDA- and AMPA-type glutamate receptors, $GABA_B$ receptor, and LGI1. However, it remains unclear how many synaptic autoantigens are yet to be defined. Using immunoproteomics, we identified autoantibodies against the $GABA_A$ receptor in human sera from two patients diagnosed with encephalitis who presented with cognitive impairment and multifocal brain MRI abnormalities. Both patients had antibodies directed against the extracellular epitope of the β3 subunit of the $GABA_A$ receptor. The β3-subunit-containing $GABA_A$ receptor was a major target of the patients' serum antibodies in rat hippocampal neurons because the serum reactivity to the neuronal surface was greatly decreased by 80% when the β3 subunit was knocked down. Our developed multiplex ELISA testing showed that both patients had similar levels of $GABA_A$ receptor antibodies, one patient also had a low level of LGI1 antibodies, and the other also had CASPR2 antibodies. Application of the patients' serum at the time of symptom presentation of encephalitis to rat hippocampal neuron cultures specifically decreased both synaptic and surface $GABA_A$ receptors. Furthermore, treatment of neurons with the patients' serum selectively reduced miniature IPSC amplitude and frequency without affecting miniature EPSCs. These results strongly suggest that the patients' $GABA_A$ receptor antibodies play a central role in the patients' symptoms. Therefore, this study establishes anti-$GABA_A$ receptor encephalitis and expands the pathogenic roles of $GABA_A$ receptor autoantibodies.

Key words: autoantibody; autoimmune encephalitis; cognitive impairment; $GABA_A$ receptor; seizure; thymoma

Introduction

Autoimmune neurological disorders are induced through the production of autoantibodies. Identifying the target antigens and elucidating the pathogenic mechanisms of autoantibodies play extremely important roles in the diagnosis and treatment of autoimmune disorders (Vincent et al., 2006; Moscato et al., 2010; Lancaster and Dalmau, 2012). In particular, autoantibodies to synaptic cell surface antigens have attracted considerable attention because such antibodies may be directly pathogenic by interfering with synaptic functional proteins.

In the CNS, antibodies to the metabotropic glutamate receptor 1, which cause cerebellar ataxia, were found in two patients with Hodgkin's disease (Sillevis Smitt et al., 2000). Antibodies to the ionotropic NMDA-type glutamate receptor were then identified in many patients with ovarian tumors, psychiatric symptoms, amnesia, seizures, and impaired consciousness (Dalmau et al., 2007). This disease has since been established as "anti-NMDA receptor encephalitis" (Dalmau et al., 2008). Since 2009, immunoprecipitation coupled with mass spectrometry analysis using patient serum antibodies has accelerated the identification of target antigens associated with limbic encephalitis characterized by subacute onset of amnesia and seizures. Another major ionotropic glutamate receptor, the AMPA receptor (Lai et al., 2009), the inhibitory metabotropic $GABA_B$ receptor (Lancaster et al., 2010), and CASPR2 and LGI1, which were previously recognized as the voltage-gated potassium channel (VGKC) (Irani et al., 2010; Lai et al., 2010), were identified as cell surface autoantigens in patients with limbic encephalitis. In addition, antibodies to inhibitory ionotropic glycine receptor were reported in a spec-

Received Oct. 15, 2013; revised April 25, 2014; accepted May 5, 2014.

Author contributions: T. Ohkawa, Y.F., and M.F. designed research; T. Ohkawa, S.S., Y.F., and M.F. performed research; N.Y., Y.M., T. Ohshita, G.S., H.T., O.W., Y.F., and M.F. contributed unpublished reagents/analytic tools; T. Ohkawa, S.S., O.W., Y.F., and M.F. analyzed data; T. Ohkawa, Y.F., and M.F. wrote the paper.

This work was supported by the Ministry of Education, Culture, Sports, Science and Technology (Grant 25110733 to Y.F. and Grant 25461286 to O.W.); the Ministry of Health, Labour and Welfare (Intramural Research Grant H24-12 for Neurological and Psychiatric Disorders of NCNP to Y.F., Grant 24133701, and Research on Measures for Intractable Diseases Grant H24-017 to O.W.); and the Cabinet Office (Funding Program for Next Generation World-Leading Researchers Grant LS123 to M.F.). We thank K. Imoto and H. Furue for encouragement and helpful suggestions; B. Lüscher for a plasmid encoding $GABA_A$ receptor γ2; the members of the Fukata and Takashima laboratories, Y. Shirahama, T. Kohriyama, and K. Ochi for kind support; all of the physicians who provided serum samples and clinical information from the patients; and all of the patients and their families.

The authors declare no competing financial interests.

Correspondence should be addressed to either Yuko Fukata or Masaki Fukata, Division of Membrane Physiology, Department of Cell Physiology, National Institute for Physiological Sciences, National Institutes of Natural Sciences, 5-1 Higashiyama, Myodaiji, Okazaki, Aichi 444-8787, Japan, E-mail: yfukata@nips.ac.jp or mfukata@nips.ac.jp.

*Y.F. and M.F. contributed equally to this work.

DOI:10.1523/JNEUROSCI.4415-13.2014

 0270-6474/14/348151-13$15.00/0

trum of brainstem and spinal hyperexcitability disorders (stiff-person syndrome phenotype) (Hutchinson et al., 2008; McKeon et al., 2013).

The ionotropic GABA$_A$ receptor mediates most of the fast inhibitory synaptic transmission in the brain and is composed of heteropentameric assemblies of different subunit subtypes [α (1–6), β (1–3), γ (1–3), δ, ε, θ, π, and ρ (1–3)] to form chloride ion channels (Macdonald and Olsen, 1994; Jacob et al., 2008; Rudolph and Knoflach, 2011). The majority of GABA$_A$ receptors contain two α subunits, two β subunits, and one γ or δ subunit. The GABA$_A$ receptor plays a central role in the regulation of brain excitability and is targeted by many antiepileptic, sedative, and anxiolytic drugs, including benzodiazepines and barbiturates. In addition, mutations in human GABA$_A$ receptor subunits, including α1, β3, γ2, and δ, cause genetic epilepsy syndromes (Macdonald et al., 2010) and genetic loss of the β3 subunit in mice causes seizures and learning and memory deficits (DeLorey et al., 1998). Therefore, although the GABA$_A$ receptor can be a strong candidate affected in autoimmune CNS disorders, GABA$_A$ receptor antibodies have not yet been reported.

Here, using a nonbiased proteomic method, we identified autoantibodies against the GABA$_A$ receptor in two patients with encephalitis. The patients' GABA$_A$ receptor antibodies specifically caused downregulation of GABA$_A$ receptors. The present study establishes a pathogenic role of GABA$_A$ receptor antibodies in certain cases of encephalitis.

Materials and Methods

Experiments. The experiments using human sera were reviewed and approved by ethic committees at the National Institute for Physiological Sciences (NIPS), Nagoya University, and Kagoshima University, and written informed consent was obtained from all patients or their family members. All animal studies were reviewed and approved by the ethic committees at NIPS and were performed according to the institutional guidelines concerning the care and handling of experimental animals.

Study population and serum samples. We collected ~1200 serum samples from patients who were diagnosed with or suspected of immune-mediated disorders of the CNS or PNS. These patients were seen by us or by clinicians at other institutions in Japan. To screen for synaptic cell surface autoantigens, we selected serum samples from 116 patients diagnosed with or suspected of immune-mediated encephalitis (59 males and 57 females), which included 76 limbic encephalitis, 24 encephalitis, nine encephalopathy, four anti-NMDA receptor encephalitis, and three Hashimoto encephalopathy cases. These patients presented with subacute onset of some CNS symptoms, including cognitive impairment, confusion/disorientation, and/or seizures. For the first screening, these 116 samples with encephalitis (and also 49 samples with other immune-mediated neurological disorders described in the following sentence) were tested for binding to the cell surface of cultured rat hippocampal neurons. For the second round of screening for binding to the cell surface of COS7 cells expressing the GABA$_A$ receptor, we tested serum samples from all of the 116 patients with encephalitis and an additional 94 control subjects (54 males and 40 females): 49 patients (32 males and 17 females) with or suspected of other immune-mediated neurological disorders, including 35 neuromyotonia, six cramp-fasciculation syndrome, three myasthenia gravis, two Morvan syndrome, one stiff-person syndrome, one Guillain-Barre syndrome, and one chronic inflammatory demyelinating polyneuropathy case; 22 patients (10 males and 12 females) with neurodegenerative diseases, including seven amyotrophic lateral sclerosis, six spinocerebellar degeneration, five multiple system atrophy, two Parkinson's disease, one corticobasal degeneration, and one frontotemporal lobar degeneration case; and 23 healthy individuals (12 males and 11 females). The study population and control subjects contained 19 patients with the complications of thymoma (including 12 invasive thymoma cases). The serum samples of Patient 1 and Patient 2 used for the present screening were both from their initial episodes of encephalitis (Table 1). Due to the current unavailability of patients' CSF samples, only the serum samples were used in the present study.

Antibodies. The antibodies used in this study included the following: rabbit polyclonal antibodies to GABA$_A$ receptor α2 (catalog #600-401-D45 RRID:AB_11182018; Rockland Immunochemicals), α5 (catalog #AB9678 RRID:AB_570435; Millipore), β3 (catalog #ab4046 RRID:AB_2109564; Abcam), γ2 (extracellular epitope, catalog #224 003 RRID:AB_2263066; Synaptic Systems), and AMPA receptor GluA1 (catalog #AB1504 RRID:AB_2113602; Millipore; and extracellular epitope, catalog #PC246-100UG RRID:AB_564636; Millipore); guinea pig polyclonal antibodies to vGAT (catalog #131 005 RRID:AB_1106810; Synaptic Systems) and vGluT1 (catalog #AB5905 RRID:AB_2301751; Millipore); and mouse monoclonal antibodies to GABA$_A$ receptor α1 (catalog #75-136 RRID:AB_2108811; NeuroMab), β1 (catalog #75-137 RRID:AB_2109406; NeuroMab), β2/β3 (extracellular epitope, catalog #MAB341 RRID:AB_2109419; Millipore), β-catenin (catalog #610153 RRID:AB_397554; BD Biosciences), gephyrin (catalog #147 021 RRID:AB_1279448; Synaptic Systems), PSD-95 (catalog #MA1-046 RRID:AB_2092361; Thermo Scientific), and N-cadherin (catalog #610921 RRID:AB_398236; BD Biosciences).

Plasmid construction. The cDNAs of rat GABA$_A$ receptor α1 (NM_183326), α2 (NM_001135779), α5 (NM_017295), β1 (NM_012956), and β3 (NM_017065) were cloned from rat brain total RNA by RT-PCR. These cDNAs were subcloned into pCAGGS vector. Dr. Bernhard Lüscher (Pennsylvania State University) kindly provided pRK5:Myc-mouse GABA$_A$ receptor γ2 (Fang et al., 2006).

Rat GABA$_A$ receptor β3 subunit was knocked down by the miR-RNAi system (Life Technologies). BLOCK-iT RNAi Designer was used to select the targeting sequences and the following targeting sequences were used: miR-β3-211, 5′-AGCATCGACATGGTTTCTGAA-3′ (an alternative sequence: miR-β3-347, 5′-TCTGGGTGCCTGACACATATT-3′; both sequences yielded the same results) and miR-LacZ (β-galactosidase), 5′-GACTACACAAATCAGCGATTT-3′ as a negative control. After subcloning these oligonucleotides into pcDNA6.2-EmGFP-miR, the pre-miRNA expression cassette of pcDNA6.2-EmGFP-miR was transferred to pCAGGS vector with a β-actin promoter. The resultant miR constructs were validated for the knock down of cotransfected rat GABA$_A$ receptor β3 expression in HEK293T cells by Western blotting (see Fig. 3*A*). Rat GABA$_A$ receptor β3 subunit rescue construct [miR-β3-211-resistant β3 (resβ3) in pCAGGS], which has two different nucleotides in the target sequences, was generated using site-directed mutagenesis (5′-AACATCGACATCGCCAGCAT*TG*GA*T*ATGGTTTCTGAAGTCAA-CAT-3′; changed nucleotides are shown in italic font). All PCR products were analyzed by DNA sequencing (Functional Genomics Facility, National Institute for Basic Biology).

Immunofluorescence analysis of cultured hippocampal neurons. Cultured rat hippocampal neurons (5×10^4 cells) were obtained from embryonic day 18–19 embryos and seeded onto poly-L-lysine-coated 12 mm coverslips in 24 well dishes. For selecting the serum samples that bind to neuronal cell surface, live neurons (21–28 DIV) were incubated with the serum from 116 patients diagnosed with or suspected of immune-mediated encephalitis for 1 h at 37°C (diluted 1:100). The neurons were subsequently fixed with 4% paraformaldehyde/120 mM sucrose/100 mM HEPES, pH 7.4, at room temperature for 10 min and blocked with PBS containing 10 mg/ml BSA for 15 min. The bound human Ig (IgG) was visualized using Cy3-conjugated secondary antibody. For Figure 1*D*, live neurons were incubated with the patient serum (diluted 1:200) together with anti-GABA$_A$ receptor γ2 antibody (against the extracellular epitope) for 30 min at 37°C. The neurons were fixed and labeled by Cy3-conjugated human IgG and Alexa Fluor 488-conjugated rabbit IgG antibodies. The neurons were then permeabilized and incubated with anti-gephyrin antibody, followed by staining with Alexa Fluor 647-conjugated mouse IgG antibody.

For Figure 3, knock down of the GABA$_A$ receptor β3 subunit was performed using the miR-RNAi system as described previously (Fukata et al., 2013). Briefly, hippocampal neurons (10 DIV) were transfected with the knock-down vector (miR-LacZ or miR-β3) with or without rescue β3 construct by Lipofectamine 2000. At 5 d after transfection, live

neurons were incubated with anti-$GABA_A$ receptor $\beta2/\beta3$ subunit antibody (against the extracellular epitope) or the patient serum (diluted 1:200) together with anti-$\gamma2$ subunit antibody (against the extracellular epitope) for 30 min at 37°C. The neurons were fixed and blocked with PBS containing 10 mg/ml BSA for 30 min on ice. The $\beta3$ subunit or the bound human IgG and $\gamma2$ were visualized using Cy3-conjugated and Alexa Fluor 647-conjugated secondary antibodies, respectively. Neurons transfected with the knock-down vector were reported by co-cistronic expression of EmGFP. To quantify the effect of the knock down (Fig. 3*D*), we randomly chose neurons from two separate cultures and made the intensity profile along the lines (total ~100 μm in length) in somatodendritic regions (LAS AF software; Leica Microsystems). The number of clusters labeled by $\beta2/\beta3$ antibody or human IgG (threshold was set at 1000 arbitrary units of mean fluorescent intensity) was counted. Because the expression of rescue $\beta3$ construct enhanced fluorescence intensity of the clusters, the images of miR-$\beta3$-211 + res$\beta3$-transfected neurons were acquired with 50% of laser power used for miR-LacZ + GST- or miR-$\beta3$-211 + GST-transfected neurons (GST was used as a mock vector).

For Figures 1*D* and 3, fluorescent images were captured with a confocal laser scanning microscopy system (TCS SP5 II; Leica) equipped with an HCX Plan Apochromat 63×/1.40 numerical aperture (NA) oil-immersion objective lens combining with the Leica HyD detectors. For Figures 2, 4, and 5, images were captured with a system (LSM5 Exciter; Carl Zeiss) equipped with a Plan Apochromat 63×/1.40 NA oil-immersion objective lens.

Immunoprecipitation and mass spectrometry. Rat hippocampal neurons (5×10^5 cells/well) were seeded in six well plates. The neurons were incubated with the patient serum (diluted 1:50) for 1 h at 37°C. The neurons were washed and subsequently lysed with buffer A containing the following: 20 mM Tris-HCl, pH 8.0, 1 mM EDTA, 100 mM NaCl, 1.3% Triton X-100, and 50 μg/ml PMSF. The lysates were cleared by centrifugation at 10,000 × *g* for 5 min at 4°C. The immune complexes were precipitated with Protein A Sepharose (GE Healthcare). The immunoprecipitates were separated by SDS-PAGE and the gels were subsequently analyzed by silver staining and Western blotting. All of the specific protein bands were excised from a silver-stained gel and analyzed with liquid chromatography-tandem mass spectrometry (LC-MS/MS) as described previously (Fukata et al., 2010). The gel pieces with the corresponding molecular weights in the control serum sample were also analyzed to rule out nonspecific binding to human serum antibodies.

Cell-based binding assay. COS7 cells were transfected with the indicated $GABA_A$ receptor subunits. Twenty-four hours after transfection, the cells were fixed with 4% paraformaldehyde/120 mM sucrose/100 mM HEPES, pH 7.4, at room temperature for 10 min and blocked with PBS containing 10 mg/ml BSA for 15 min. The fixed cells were incubated with the patient serum (diluted 1:10), followed by staining with the Cy3-conjugated secondary antibody. The cells were then permeabilized with 0.1% Triton X-100 for 10 min, blocked with PBS containing 10 mg/ml BSA, and incubated with antibodies to individual $GABA_A$ receptor subunits, followed by staining with the Alexa Fluor 488-conjugated secondary antibody. For the second round of screening, serum samples from all of the 116 patients with encephalitis and 94 control subjects were tested for binding to COS7 cells expressing the $GABA_A$ receptor $\alpha1/\beta3/\gamma2$ subunits. We confirmed that any serum samples did not bind to untransfected cells that did not express the $GABA_A$ receptor subunits through distinguishing untransfected cells with Hoechst dye (33342; Invitrogen) nucleic acid staining (Figs. 2*A*, 4*A*) and that neither the patient sera nor the control sera bound to COS7 cells that had not been treated with Lipofectamine transfection reagent (data not shown). To quantify the intensity of bound human IgG (Fig. 2*B*), we randomly chose 10 cells and measured the mean intensities in green and red channels. The ratio of the human IgG intensity to the $GABA_A$ receptor subunit intensity was graphed.

The identities of human and rat $GABA_A$ receptor $\alpha1$, $\beta3$, and $\gamma2$ subunits in their amino acid sequence are 100%, 97%, and 99%, respectively; and that of the human and mouse $\gamma2$ subunit is 99%, suggesting that the results obtained by using rat or mouse $GABA_A$ receptor constructs and rat neurons do not affect the interpretation of our results. Cell-based binding assay for LGI1, CASPR2, and DCC (Fig. 4*A*) was described previously (Ohkawa et al., 2013).

Cell-based ELISA. Cell-based ELISA testing for LGI1, CASPR2, and DCC was described previously (Ohkawa et al., 2013) and the ELISA testing for the $GABA_A$ receptor $\beta3$ subunit basically followed this procedure. Briefly, plasmids (0.1 μg/well for LGI1, CASPR2, and $\beta3$; 0.06 μg/well for DCC) were lipofected into HEK293T cells grown in polyethylenimine-coated 96-well plates (3×10^4 cells/well; Nunclon TC; Nunc). After a 24 h incubation, the cells were treated with the serially diluted sera (1:50, 150, 450, and 1350) from patients and control subjects together in the same plate for 15 min at 37°C. The cells were washed and fixed with 4% paraformaldehyde for 15 min. After washing and blocking, the cells were incubated with an HRP-conjugated anti-human IgG antibody in a 1:2000 dilution for 15 min at 37°C. After washing, the cell-bound human IgG was detected using Ultra-TMB substrate solution (Thermo Scientific). The colorimetric reaction was stopped upon the addition of 2 M sulfuric acid and the resulting plates were measured at 450 nm absorption with MULTISKAN FC microplate reader (Thermo Scientific). Wells containing nontransfected cells were used to subtract the background signals. The absorbance at a dilution of 1:50 was used as the antibody value for an individual patient. We previously determined the best cutoff point to predict the patient with limbic encephalitis from LGI1-ELISA values using a receiver operating characteristic curve composed of sensitivity and false-positive rate (Ohkawa et al., 2013). We showed that the ELISA test for LGI1 is useful for the diagnosis of limbic encephalitis with high specificity (94.2%), sensitivity (49.2%), and positive predictive value (85.3%) at the 0.8 cutoff point and that the ELISA for CASPR2 is useful for the diagnosis of neuromyotonia with high specificity (96.5%), sensitivity (26.7%), and positive predictive value (66.7%) at the 0.3 cutoff point (Ohkawa et al., 2013).

Tests of effects of $GABA_A$ receptor autoantibodies. To determine the effect of the patients' serum antibodies on the surface or synaptic $GABA_A$ receptor density, cultured rat hippocampal neurons (~30 DIV) were treated with the indicated serum samples for 2 d. 4.5 μl of the serum was added daily to 300 μl of each culture medium (final 3% concentration). After washing, live neurons were then incubated with an antibody to an extracellular epitope of $GABA_A$ receptor $\gamma2$ for 15 min at 37°C. After fixation, the surface-expressed $\gamma2$ subunit was visualized with the Cy3-conjugated antibody. After permeabilizing neurons, the neurons were incubated with anti-gephyrin and vGAT antibodies, followed by staining with Alexa Fluor 488- and Alexa Fluor 647-conjugated secondary antibodies, respectively. Serum-treated sister cultures were also independently stained with anti-$GABA_A$ receptor $\beta3$ subunit antibody (the intracellular epitope) after cell permeabilization to visualize the $GABA_A$ receptors containing the $\beta3$ subunit. To quantify the synaptic $GABA_A$ receptors, we randomly chose dendrites and analyzed the number of $GABA_A$ receptor $\gamma2$ and $\beta3$ clusters along dendrites (20 μm length). Three to 10 neurons were examined from each separate culture. Synaptic $\gamma2$ and $\beta3$ clusters that were adjacent to both vGAT and gephyrin and bigger than $1/\pi$ μm in diameter (threshold was set at 70 arbitrary units of mean fluorescent intensity) were counted. The quantification of gephyrin clusters apposed to vGAT was analyzed by the same criteria. The quantification of synaptic AMPA receptor was described previously (Ohkawa et al., 2013).

Biotinylation of cell surface proteins was performed as described previously (Hughes et al., 2010). Briefly, neurons were incubated with 2.3 mM Sulfo-NHS-Biotin (Thermo Scientific) for 30 min at 4°C. Neurons were then incubated with quenching buffer containing 100 mM glycine for 30 min and lysed in buffer B containing the following: 20 mM Tris-HCl, pH 8.0, 1 mM EDTA, 100 mM NaCl, 1% SDS, and 50 μg/ml PMSF. After a 20 min extraction, the lysates were diluted with 10 volumes of buffer B containing 1% Triton X-100 instead of SDS. After centrifugation at 20,000 × *g* for 20 min, the supernatant was incubated with NeutrAvidin agarose beads (Thermo Scientific) for 12 h at 4°C. The isolated surface proteins were separated by SDS-PAGE and analyzed by Western blotting with indicated antibodies. For the quantification, ImageJ software was used.

Electrophysiology. Cultured rat hippocampal neurons (1.5×10^4 cells) were seeded onto poly-L-lysine-coated 12 mm coverslips in 24 well dishes. Neurons (33–46 DIV) were treated with control serum or patients' serum samples containing $GABA_A$ receptor antibodies for 24 h.

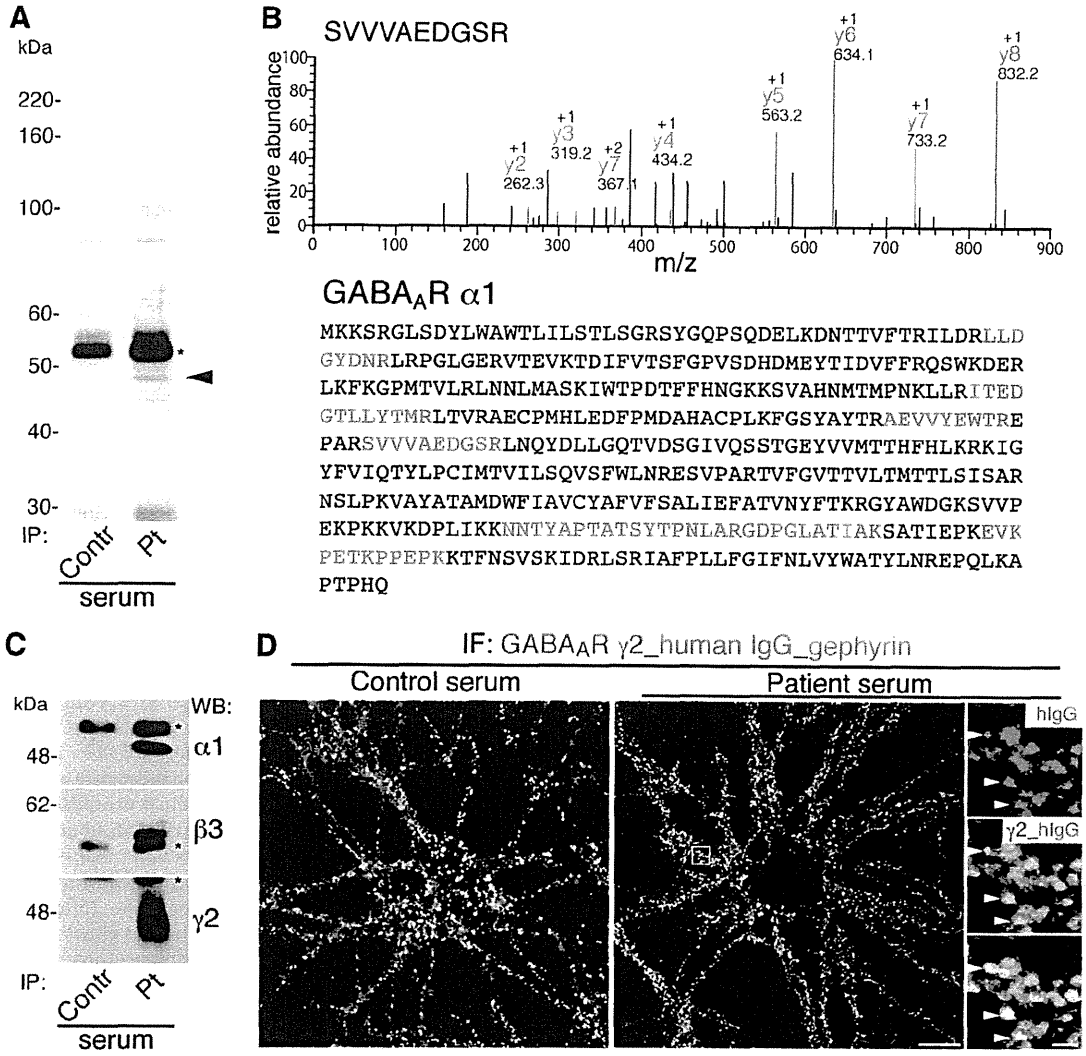

Figure 1. Identification of GABA$_A$ receptor autoantibodies in a patient with autoimmune encephalitis. ***A***, Immunoprecipitation of cell surface target proteins with patient's serum antibodies. The immunoprecipitates of serum antibodies bound to rat hippocampal neurons were analyzed by SDS-PAGE with silver staining. The specific band at 48 kDa (arrowhead) was analyzed by the LC-MS/MS. ***B***, MS/MS spectra of a peptide unique for the GABA$_A$ receptor α1 subunit (*m/z* value of the parent ion, 509.74) obtained from the trypsinized protein band shown in ***A*** (arrowhead). The matched fragment y^+ ion series is indicated in red. Identified peptides in the amino acid sequence of GABA$_A$ receptor α1 are indicated in red. The accession number is P62813. The patient serum used came from the initial episode of encephalitis of Patient 1. ***C***, Western blotting with the subunit specific antibodies showed that the α1, β3, and γ2 subunits of the GABA$_A$ receptor were present in the immunoprecipitate by the patient serum antibodies. Asterisks indicate the position of the human IgG heavy chain (***A***, ***C***). ***D***, Patient serum antibodies bind to the inhibitory GABA$_A$ receptors at the cell surface of rat hippocampal neurons. The serum reactivity (red; human IgG) was well overlapped with surface-expressed γ2 subunits of GABA$_A$ receptor (green), which were apposed to gephyrin scaffold (blue; marked by arrowheads). Magnified view of the region indicated by a white square. Scale bars, 10 μm (1 μm, magnified). IP, immunoprecipitation; Contr, control; Pt, patient; GABA$_A$R, GABA$_A$ receptor; WB, Western blotting; IF, immunofluorescence; hIgG, human Ig.

Nine microliters of the serum was added to 300 μl of the culture medium (final 3% concentration). The culture slips were transferred to a recording chamber mounted on the microscope stage (BX51WI; Olympus) and continuously superfused with an artificial CSF (ACSF) containing the following (in mM): 138.6 NaCl, 3.35 KCl, 2.5 $CaCl_2$, 1.0 $MgCl_2$, 21.0 $NaHCO_3$, 0.6 NaH_2PO_4, and 10.0 glucose equilibrated with 95% O_2 and 5% CO_2, pH 7.4, at room temperature. Flow rate was 1.0 ml/min and all experiments were performed at room temperature. Synaptic currents were recorded from the hippocampal neurons by whole-cell voltage clamping (Satake and Imoto, 2014) under Nomarski optics with a water-immersion objective (63×/0.90 NA; Olympus). Patch-clamp electrodes (resistance, 3–6 MΩ) were filled with an internal solution containing the following (in mM): 150.0 Cs-methanesulfonate, 5.0 KCl, 0.1 EGTA, 5.0 HEPES, 3.0 Mg-ATP, and 0.4 Na_3-GTP, pH 7.4. Membrane potential was held with a voltage-clamp amplifier (EPC-10; HEKA Elektronik) controlled by PatchMaster software (HEKA Elektronik). Currents were filtered at 3 kHz and digitized at 20 kHz. To record miniature IPSCs (mIPSCs), neurons were held at −20 mV in the presence of 1 μM tetrodotoxin (TTX), 20 μM CNQX, and 50 μM APV (Satake et al., 2004). To record AMPA-receptor-mediated miniature EPSCs (mEPSCs), neurons were held at −80 mV in the presence of 1 μM TTX, 10 μM bicuculline, and 50 μM APV. The Mini Analysis program (Synaptosoft Systems) was used to detect and measure mIPSCs and mEPSCs; the threshold for detection of events was threefold more than variance (σ^2) of basal noise. All data were obtained on age-matched sister cultures by an experimenter who was blinded with regard to serum treatment.

Statistical analysis. Statistical comparisons between two groups were performed by the Student's *t* test. Statistical comparisons between multiple groups were performed by one-way ANOVA with Tukey's *post hoc* analysis. When the sample sizes were unequal, Scheffe's *post hoc* analysis was used. For Figure 6*C*, statistical analysis of cumulative distribution of the mIPSC amplitude was performed using two-way ANOVA. Error bars indicate SEM in all figures.

Table 1. Clinical features of patients with encephalitis and $GABA_A$ receptor antibodies

			At onset of encephalitis[a]		History		Autoantibodies at onset of encephalitis				
Pt#	Age	Sex	Symptoms/signs	Brain MRI (T2)	Cancer and other remarks (age)	Autoimmune diseases (age); autoantibodies[b]	In original case report[b]	Determined in the present study	Treatment	Outcome	Reference
1	46	M	Subacute onset of aphasia, visual hallucination, and generalized seizures with delirium; residual thymoma	Multifocal signal abnormalities	Invasive thymoma (42); thymectomy, radiation, and chemotherapy (42)	MG (42); Anti-AchR, 500 nM; anti-VGKC, 63.7 pM (serum)	Anti-AchR, 130 nM; anti-VGKC, 649 pM (serum)	Anti-$GABA_AR$, anti-LGI1, and anti-DCC (serum)	Corticosteroids and IVIg; AED	Epileptic seizures disappeared; severe cognitive impairment and psychological symptoms remained	Miyazaki et al., 2012
2	59	F	Subacute onset of amnesia (short-term memory impairment), disorientation, and no evidence of recurrent thymoma; 10 months later, progressive memory impairment and recurrence of thymoma	Multifocal signal abnormalities in the medial temporal lobe, insular cortex, frontobasal cortex, and cingulated gyrus	Invasive thymoma (56); thymectomy and radiation (56); carbamazepine (200 mg/d) for postherpetic neuralgia (57–63)	NA	Anti-AchR, anti-Hu, and anti-Yo, negative; anti-VGKC, 403 pM (serum)	Anti-$GABA_AR$, anti-CASPR2, and anti-DCC (serum)	Chemotherapy for recurrent thymoma (carboplatin and etoposide)	Mental state partially improved	Ohshita et al., 2006

[a]The serum samples at the onset of encephalitis were used for the present screening.

[b]Anti-VGKC, normal <100 pM; anti-AchR, normal <0.2 nM.

MG, Myasthenia gravis; AchR, acetylcholine receptor; IVIg, intravenous immunoglobulin; AED, antiepileptic drug; NA, not applicable.

Results

Identification of $GABA_A$ receptor autoantibodies in patients with encephalitis

To identify novel cell surface autoantigens involved in autoimmune encephalitis, we analyzed serum samples from 116 patients with or suspected of immune-mediated encephalitis (see Study Population section in Materials and Methods). We first screened serum antibodies for binding to the cell surface of cultured rat hippocampal neurons. The serum antibodies from 37 patients bound to the neuronal cell surface (data not shown). Target proteins were immunoprecipitated from cultured neurons with the bound serum antibodies and identified by mass spectrometry. We found the previously reported autoantibodies to LGI1, AMPA receptor, CASPR2, DPP10, and DCC in patients with encephalitis (data not shown) (Lai et al., 2009; Irani et al., 2010; Lai et al., 2010; Ohkawa et al., 2013). In addition, a protein with a molecular mass of 48 kDa (p48) was specifically detected in the immunoprecipitate by serum antibodies from one patient (Fig. 1*A*), who was originally diagnosed as having invasive thymoma with the complications of myasthenia gravis and then developed encephalitis associated with VGKC-complex antibodies (Patient 1, Table 1) (Miyazaki et al., 2012). The molecular identity of p48 was determined by LC-MS/MS (Fig. 1*B*). Molecular weights of seven peptide fragments derived from p48 coincided with those from the rat $GABA_A$ receptor α1 subunit: LLDGYDNR, ITEDGTLLYTMR, AEVVYEWTR, SVVVAEDGSR, NNTYAPTATSYTPNLAR, GDPGLATIAK, and EVKPETKPPEPK. The estimated molecular weight of rat $GABA_A$ receptor α1 (51.7 kDa) was close to that of p48. In addition, peptide fragments coinciding with those from the $GABA_A$ receptor β3 subunit (NVVFATGAYPR and IKIPDLTDVNAIDR) were present in the same immunoprecipitate (the corresponding band at 54.2 kDa was masked by the human IgG heavy chain). Western blotting with antibodies specific to the α1, β3, and γ2 subunits of $GABA_A$ receptor confirmed the immunoprecipitation of heteromeric $GABA_A$ receptors (Fig. 1*C*). Consistently, the serum antibodies showed overlapped signals with inhibitory synapses marked by $GABA_A$ receptor γ2 and gephyrin antibodies in rat hippocampal neurons (Fig. 1*D*).

$GABA_A$ receptor autoantibodies are directed to extracellular epitope of the β3 subunit

To determine whether the patient serum antibodies bind directly to the $GABA_A$ receptor and, if so, which of $GABA_A$ receptor subunits the antibodies recognize, the cell-based binding assay was performed. Because the native $GABA_A$ receptor is a heteropentamer composed of two α, two β, and one γ subunits and the patient serum immunoprecipitated α1, β3, and γ2 subunits from hippocampal neurons (Fig. 1*C*), α1, β3, and γ2 subunits were coexpressed to display heteropentameric $GABA_A$ receptors at the cell surface of COS7 cells. Transfected cells were then fixed and incubated with the patient serum without cell permeabilization. We found that the serum antibodies from Patient 1 robustly reacted to the surface-expressed $GABA_A$ receptors (α1/β3/γ2; Fig. 2*A*, left). Among 19 individual $GABA_A$ receptor subunits, we then examined the binding to individual $GABA_A$ receptor subunits (α1, α2, α5, β1, β3, and γ2), which are known to be included in $GABA_A$ receptor heteromers expressed in hippocampus (Pirker et al., 2000). The serum antibodies from Patient 1 strongly reacted to the cells expressing the β3 subunit alone and weakly reacted to those expressing the γ2 subunit alone, but did not to those expressing the α1, α2, α5, or β1 subunit alone (Fig. 2*A*,*B*). Then, as the second round of screening, we tested serum samples from all of the 116 patients with encephalitis for binding to the cell surface of COS7 cells expressing the $GABA_A$ receptor (α1/β3/γ2). We additionally tested serum samples from 94 control subjects (see Materials and Methods). We found that another patient (Patient 2) diagnosed with encephalitis had antibodies against the $GABA_A$ receptor α1/β3/γ2 and that the antibodies also strongly recognized the β3 subunit, but neither the α1 nor the γ2 subunit (Fig. 2*A*,*B*). Patient 2 had invasive thymoma and limbic encephalitis associated with VGKC-complex antibodies (Ohshita et al., 2006) (Table 1). Therefore, the common clinical features between two patients with $GABA_A$ receptor antibodies are cognitive impairment, multifocal abnormal brain MRI signals, and invasive thymoma. Patient 1 had seizures/status epilepticus, but Patient 2 had no seizure episodes (see Discussion). We did not find any control subjects that bound to the $GABA_A$ re-

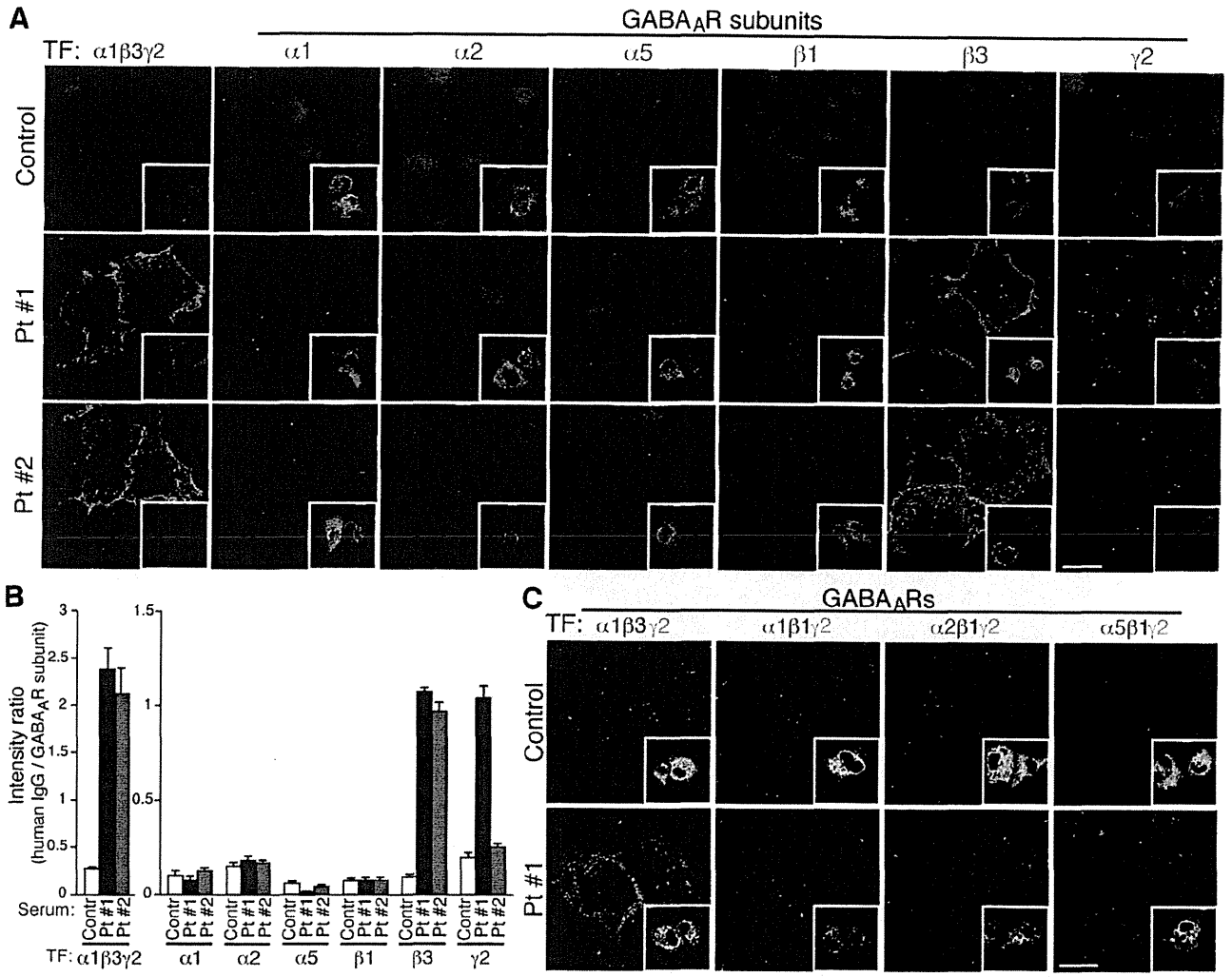

Figure 2. Patients' $GABA_A$ receptor antibodies are directed to extracellular epitope of $\beta 3$ subunit. ***A***, ***B***, COS7 cells were transfected (TF) to surface express the indicated $GABA_A$ receptor subunits. Transfected cells were fixed and doubly stained with the patient sera (Patient 1 or Patient 2; red, human IgG) together with the antibodies specific to the individual expressed subunits (green, insets). Nuclear DNA was stained by Hoechst 33342 (blue) to distinguish untransfected cells. To clearly show the weak binding of the serum from Patient 1 to the $\gamma 2$ subunit, the detector gain of the red channel is enhanced upon image acquisition (right, middle). The ratio of the human IgG intensity to the $GABA_A$ receptor subunit intensity was graphed (***B***). Error bars indicate SEM; $n = 10$ transfected cells. ***C***, COS7 cells were transfected to surface express the indicated heteromeric $GABA_A$ receptors and tested for binding of serum antibodies (red). Transfected cells were detected by staining with the individual α subunit (green) and $\gamma 2$ subunit (blue) antibodies. Merged images are shown in insets. Scale bars, 20 μm.

ceptor ($\alpha 1/\beta 3/\gamma 2$; a representative is shown in Fig. 2*A*), although this screening might have missed some serum samples that contained antibodies to other $GABA_A$ receptor subunits than $\alpha 1/\beta 3/\gamma 2$. Because neither serum antibody from the two patients bound to COS7 cells expressing the α subunit alone, one may wonder whether the α subunit might not have been efficiently expressed at the cell surface without other subunits. To further examine the possible involvement of α subunit antibodies in the patient serum, COS7 cells were transfected with various combinations of three subunit genes of the $GABA_A$ receptor, $\alpha 1/\beta 3/\gamma 2$, $\alpha 1/\beta 1/\gamma 2$, $\alpha 2/\beta 1/\gamma 2$, or $\alpha 5/\beta 1/\gamma 2$ (Fig. 2*C*). There were no apparent differences in the weak binding of serum antibodies from Patient 1 to three different $GABA_A$ receptors, $\alpha 1/\beta 1/\gamma 2$, $\alpha 2/\beta 1/\gamma 2$, and $\alpha 5/\beta 1/\gamma 2$, indicating that the binding of serum antibodies was attributed to the $\gamma 2$ subunit, but not to the $\alpha 1$, $\alpha 2$, or $\alpha 5$ subunits. Serum from Patient 2 did not show any apparent binding to $\alpha 1/\beta 1/\gamma 2$, $\alpha 2/\beta 1/\gamma 2$, or $\alpha 5/\beta 1/\gamma 2$ (data not shown). Together, these results indicate that the two patients with immune-mediated encephalitis had autoantibodies directed against the $GABA_A$ receptor and that the extracellular part of the $\beta 3$ subunit was the antigenic epitope recognized by the patients' $GABA_A$ receptor antibodies. One of the two patients also had a low level of $\gamma 2$ autoantibodies (Patient 1), but neither patient had any autoantibodies to the $\alpha 1$, $\alpha 2$, $\alpha 5$, or $\beta 1$ subunit.

$GABA_A$ receptor containing $\beta 3$ subunit is the main target of the patient serum antibodies

We next investigated whether the $GABA_A$ receptor is the main target of the patient serum antibodies in neurons. We took advantage of knock-down approach in cultured rat hippocampal neurons. MicroRNAs (miRNA-$\beta 3$-211 and miRNA-$\beta 3$-347) for the $GABA_A$ receptor $\beta 3$ subunit were first validated by the reduced expression of exogenously expressed rat $GABA_A$ receptor $\beta 3$ in HEK293T cells (Fig. 3*A*). Then, by cell surface staining with anti-$\beta 2/\beta 3$ antibody, we quantified the knock-down effect on the $\beta 3$ subunit expression in neurons. When miRNA-$\beta 3$-211 for the $GABA_A$ receptor $\beta 3$ subunit was expressed in neurons, the number of $\beta 3$ subunit clusters in soma and dendrites that were stained

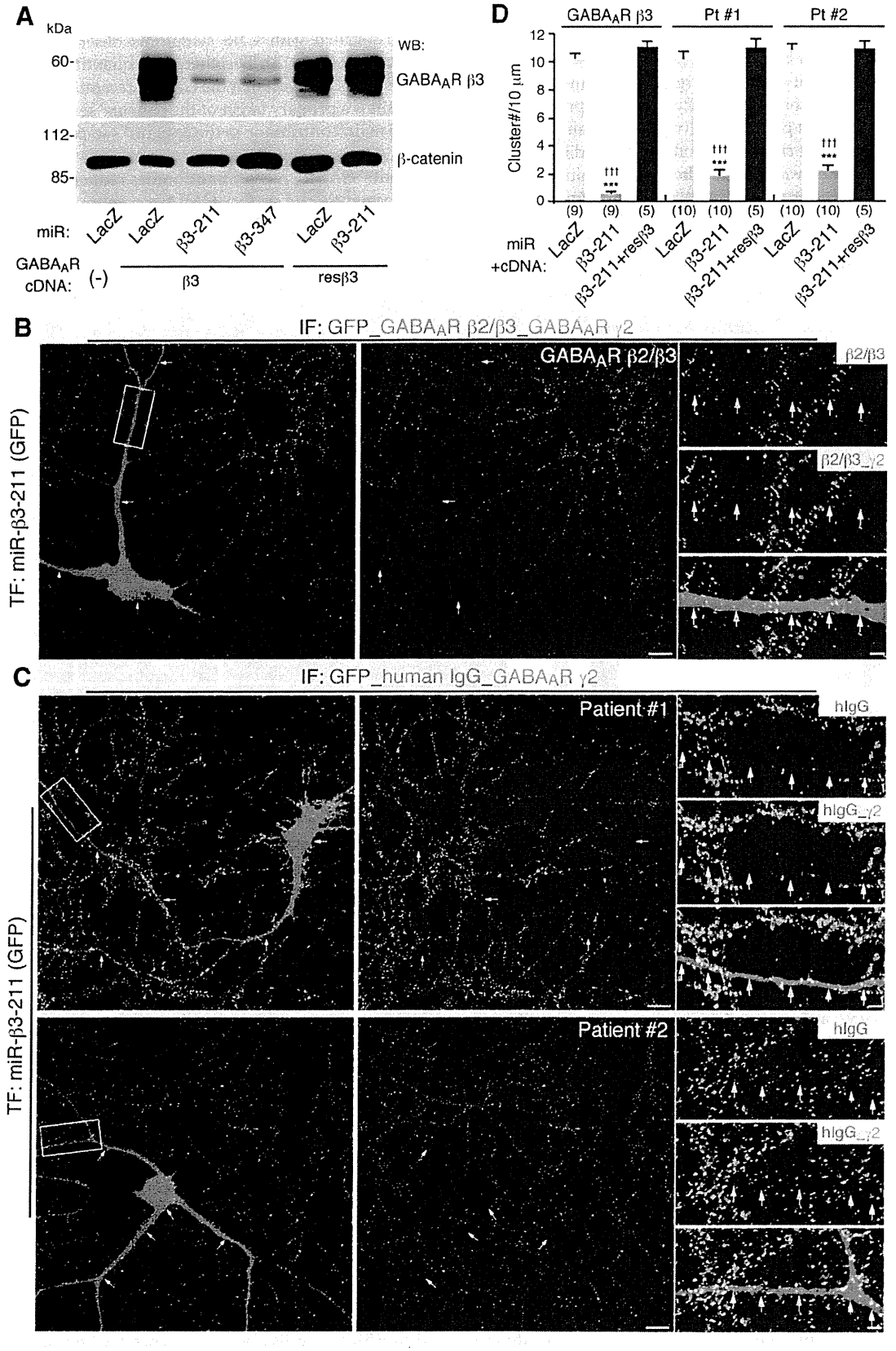

Figure 3. GABA$_A$-receptor-containing β3 subunit is a major target of the patients' antibodies in hippocampal neurons. ***A***, Validation of miRNA constructs for the GABA$_A$ receptor β3 subunit. HEK293T cells were cotransfected with the indicated knock-down (miR) and β3 expression vectors. Three days after the transfection, the cell lysates were analyzed by Western blotting with GABA$_A$ receptor β3 and β-catenin antibodies. miR-LacZ, Control miRNA targeting to LacZ; resβ3, miR-211-resistant β3. ***B***, Effective knock down of the endogenous β3 subunit. Cultured rat hippocampal neurons were transfected with the miR-β3 expression vector at 10 DIV. Cell surface GABA$_A$ receptor β2/β3 (red) and γ2 (blue) subunits were stained at 15 DIV. (*Figure legend continues.*)

by anti-β2/β3 antibody was robustly reduced, showing that β3 subunit expression was decreased to 5.47 ± 3.60% (Fig. 3*B*,*D*). This is consistent with the previous report showing that β2 expression is very low in hippocampal neurons (Pirker et al., 2000). This reduction was not due to off-target effects of miRNA expression because it was completely rescued by coexpression of the knock-down-resistant β3 construct (resβ3) with miRNA-β3. We noted that γ2 subunit clusters were also decreased in neurons in which the β3 subunit was knocked down, confirming an essential role of the β3 subunit in the $GABA_A$ receptor function in hippocampal neurons (DeLorey et al., 1998). Under these conditions, the overall immunoreactivity of the sera from Patient 1 and Patient 2 to the neurons was greatly reduced by the expression of miRNA-β3-211 and rescued by coexpression of the knock-down-resistant β3 construct. Importantly, the residual immunoreactivity upon β3 knock down was 18.2 ± 10.8% for Patient 1 and 19.8 ± 11.7% for Patient 2 (Fig. 3*C*,*D*). These results indicate that the binding of the patients' antibodies to the neuronal surface was mostly (~80%) attributed to the $GABA_A$ receptor containing the β3 subunit and that the patients had other autoantibodies in addition to $GABA_A$ receptor antibodies.

Coexisting antibodies with $GABA_A$ receptor antibodies in the patient serum

We therefore performed the cell-based binding assay (Fig. 4*A*) and the cell-based ELISA test, which quantifies the frequent serum antibodies against LGI1, CASPR2, DCC (Ohkawa et al., 2013), and $GABA_A$ receptor β3 (Fig. 4*B*). We found that the serum samples of Patient 1 and Patient 2, but no other tested serum samples, bound to the $GABA_A$ receptor β3 (Fig. 4*A*) and showed similar positive values for $GABA_A$ receptor antibodies (ELISA absorbance = 0.57 for Patient 1; 0.52 for Patient 2; Fig. 4*B*). We also found that Patient 1 had low levels of LGI1 antibodies (absorbance = 0.37) and DCC antibodies (absorbance = 0.26) in addition to $GABA_A$ receptor antibodies, but not CASPR2 antibodies. In contrast, serum from Patient 2 contained CASPR2 antibodies (absorbance = 0.51) and a low level of DCC antibodies (absorbance = 0.21) in addition to $GABA_A$ receptor antibodies, but not LGI1 antibodies. However, the low level of LGI1 antibodies of Patient 1 is unlikely to cause the patient's CNS symptoms, because the value for LGI1 antibodies of Patient 1 was much lower than the cutoff value (absorbance = 0.8) determined for diagnosis of limbic encephalitis (Ohkawa et al., 2013; see Materials and Methods). In fact, in the present study population, patients with limbic encephalitis and monospecific LGI1 antibodies had much higher levels of LGI1 antibodies (average of ELISA absorbance = 1.41 ± 0.36, n = 34 patients; Patient A as a representative) than patients with neuromyotonia (no CNS symptoms) and LGI1 autoantibodies (0.65 ± 0.16, n = 10 patients; Patient C as a representative) (Fig. 4). CASPR2 and DCC antibodies are also unlikely to be causes of the patient's CNS symptoms because CASPR2 and DCC autoantibodies are specifically associated with PNS symptoms of neuromyotonia, but are not associated with CNS symptoms observed in encephalitis (Ohkawa et al., 2013). Together, these quantitative analyses (Figs. 3, 4) strongly suggest that the $GABA_A$ receptor containing the β3 subunit is a primary target of the patients' serum antibodies and is the main contributor to the patients' symptoms.

Patients' $GABA_A$ receptor antibodies reduce the number of both synaptic and surface $GABA_A$ receptor clusters

Next, we explored a mode of action of patients' $GABA_A$ receptor antibodies. Previous studies showed that autoantibodies against NMDA and AMPA receptors induce the internalization of the corresponding receptors and reduce the number of synaptic receptors (Lai et al., 2009; Hughes et al., 2010). These previous findings inspired us to investigate whether patients' $GABA_A$ receptor antibodies reduce the number of synaptic $GABA_A$ receptors. When hippocampal neurons were treated with the serum from Patient 1 and Patient 2 for 2 d, the number of synaptic $GABA_A$ receptor clusters, represented by γ2 or β3 subunit clusters adjacent to both gephyrin and vGAT, was significantly reduced (Fig. 5*A*). The effect was specifically attributed to the patients' $GABA_A$ receptor antibodies because treatment of neurons with a control serum without detectable autoantibodies or with the serum from the patient (Patient C) with invasive thymoma and neuromyotonia, who had LGI1 and CASPR2 antibodies but not $GABA_A$ receptor antibodies (Fig. 4), did not affect the synaptic $GABA_A$ receptor clusters. The number of surface γ2 subunit clusters, including both synaptic and extrasynaptic $GABA_A$ receptors, was also heavily reduced by treatment with the serum from Patient 1 and Patient 2. The effect of the patients' serum on $GABA_A$ receptor clusters was not complement mediated because the heat-inactivated patient serum reduced the number of both synaptic and surface $GABA_A$ receptor to a similar extent to the non-heat-inactivated patient serum; therefore, we pooled these data. Under these conditions, the number of gephyrin clusters apposed to vGAT was not altered (Fig. 5*A*). The effect of the patients' sera on $GABA_A$ receptor clusters was selective because the same treatment did not affect synaptic or surface AMPA receptor subunit GluA1.

This cell biological results were confirmed by the biochemical experiment: hippocampal neurons were treated with the patient or control serum for 3 d and then the surface-expressed proteins were labeled with biotin and purified by the avidin-conjugated beads (Fig. 5*B*). In the patient serum-treated neurons, the amount of cell surface $GABA_A$ receptor β3 subunits was significantly reduced and the total amount of the β3 subunit tended to be reduced (but not significantly). This effect was specific to the $GABA_A$ receptor because the amount of the surface GluA1 and N-cadherin was not affected. Together, these results indicate that $GABA_A$ receptor autoantibodies cause a selective decrease in $GABA_A$ receptor surface density and synaptic localization, probably by enhancing the receptor internalization.

To determine the relationship between $GABA_A$ receptor antibodies and patient' symptoms, we compared serum samples of Patient 1 at two different time points, from the episode of invasive thymoma and myasthenia gravis (without encephalitis) and from the episode of encephalitis. The sample of Patient 1 before the episode of encephalitis had acetylcholine receptor (AchR) antibodies, but no detectable $GABA_A$ receptor antibodies (Fig. 5*C*, Table 1) and showed no effects on synaptic $GABA_A$ receptor density (Fig. 5*D*). In contrast, the sample of the same patient at the time of symptom presentation of encephalitis had elevated $GABA_A$ receptor antibodies instead of AchR antibodies and decreased synaptic $GABA_A$ receptor density (Fig. 5*C*,*D*). Therefore, the clinical course of Patient 1

←

(*Figure legend continued.*) MicroRNA-transfected neurons were reported by the GFP expression (green). ***C***, Binding of serum antibodies (Patient 1 and Patient 2; red) was examined in neurons in which the β3 subunit was knocked down (green). Magnified view of the region indicated by a white square (***B***, ***C***). Arrows indicate the soma and dendrites of the neuron in which β3 was knocked down (***B***, ***C***). Scale bars, 10 μm (2 μm, magnified). ***D***, Neurons were cotransfected with the indicated miR and the knock-down-resistant construct (resβ3) or GST (for mock). The number of clusters labeled by β3 antibody or human IgG of patients' serum (Patient 1 and Patient 2) was counted and graphed. One-way ANOVA with Scheffe's *post hoc* analysis, $^{***}p < 0.001$ compared with miR-LacZ; $^{\dagger\dagger\dagger}p < 0.001$ compared with miR-β3–211 + resβ3. Error bars indicate SEM. The number of neurons examined is indicated in parentheses.

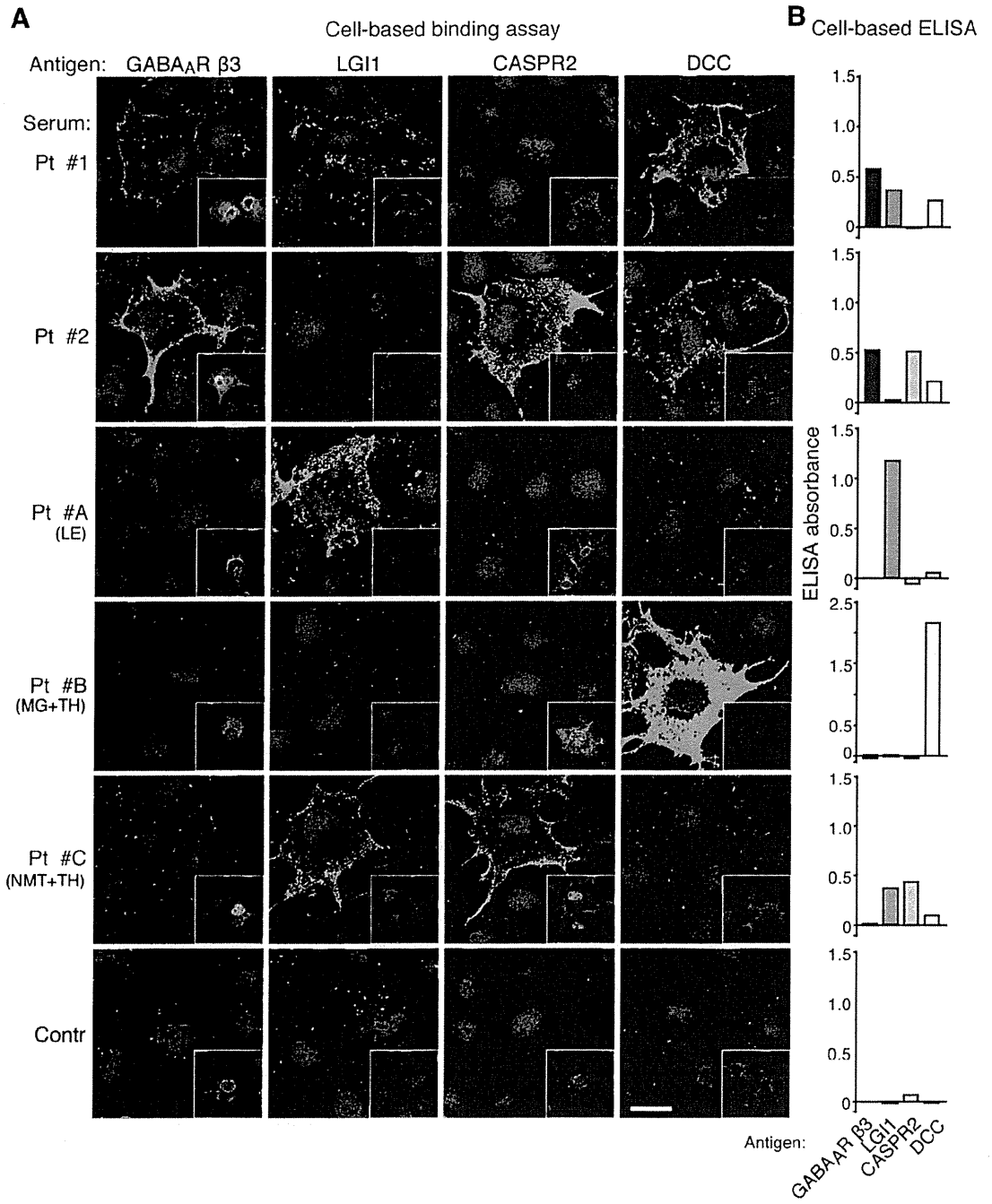

Figure 4. Identification of coexisting antibodies with GABA$_A$ receptor antibodies in the patient serum. ***A***, ***B***, Patient 1 and Patient 2 sera from their initial episodes of encephalitis were tested by cell-based binding assay (***A***) and cell-based ELISA tests (***B***) against the GABA$_A$ receptor β3 subunit, LGI1, CASPR2, and DCC. Additional sera were tested: from Patient A with limbic encephalitis (LE), Patient B with myasthenia gravis (MG) and thymoma (TH), and Patient C with neuromyotonia (NMT) and thymoma. Contr, Serum sample from a control patient with a neurodegenerative disease. Scale bar, 20 μm in ***A***. Average values from triplicate measurements of the individual serum are shown in ***B***.

correlates with the levels and effects of the patient's GABA$_A$ receptor antibodies. Although LGI1 antibodies were also detected only at the time of symptom presentation of encephalitis, the low level of LGI1 antibodies is unlikely to cause the patient's CNS symptoms, as described for Figure 4 (also see Discussion).

Patients' GABA$_A$ receptor antibodies selectively reduce mIPSC amplitude and frequency

Finally, we assessed the effects of two patient sera (Patient 1 and Patient 2) on inhibitory synaptic transmission by whole-cell patch-clamp recording of mIPSCs in rat hippocampal neurons. We found a significant decrease in the mean amplitude of mIPSCs in patients' serum-treated neurons compared with that of control serum-treated neurons (Fig. 6*A*,*B*). This result is consistent with our immunocytochemical data (Fig. 5*A*) showing that the treatment of neurons with patients' serum reduced the number of synaptic clusters of GABA$_A$ receptors. The frequency of mIPSCs was also decreased in patients' serum-treated neurons (Fig. 6*A*,*B*), probably due to the increase in small-amplitude mIPSCs that fell below the threshold of de-

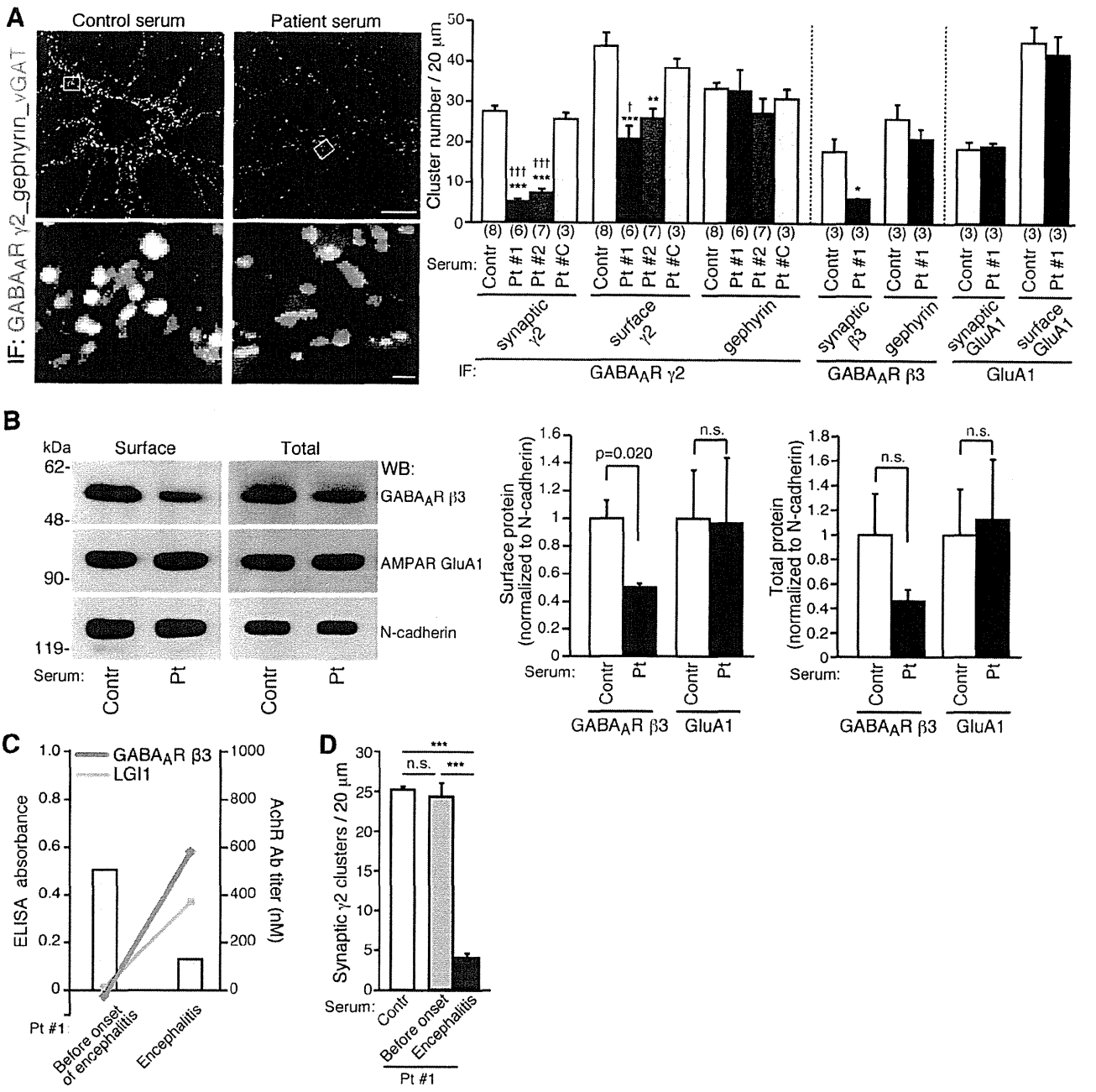

Figure 5. Patients' GABA$_A$ receptor antibodies specifically reduce synaptic and cell surface GABA$_A$ receptor density. ***A***, Cultured rat hippocampal neurons were incubated with serum from Patient 1 and Patient 2, serum from Patient C with thymoma that contained both LGI1 and CASPR2 antibodies (Fig. 4), or a control serum for 2 d. Representative images of surface GABA$_A$ receptor clusters in neurons treated with the control or the serum from Patient 1 are shown (left). Bottom, Magnified view of the region indicated by a white square. Synaptic GABA$_A$ receptors, which were γ2 (red) or β3 (data not shown) subunit-positive clusters adjacent to both gephyrin (green) and vGAT (blue), were counted. Surface-expressed GABA$_A$ receptor clusters labeled by the γ2 subunit antibody and gephyrin clusters were also independently counted. In addition, synaptic GluA1 clusters adjacent to both PSD-95 and vGluT1 and surface-expressed GluA1 clusters were counted. Scale bars, 20 μm (1 μm, magnified). Statistical analyses were performed by one-way ANOVA with Scheffe's *post hoc* analysis (γ2 clusters); or by Student's *t* test (β3 and GluA1 clusters). $*p < 0.05$; $**p < 0.01$; $***p < 0.001$ compared with control; $†p < 0.05$, $†††p < 0.001$ compared with Patient C. Error bars indicate SEM. The number of separate cultures is indicated in parentheses. ***B***, Surface biotinylated and total proteins of the serum from Patient 1 treated hippocampal neurons were analyzed by Western blotting with the indicated antibodies. Student's *t* test; n.s., not significant. Error bars indicate SEM; $n = 3$ separate cultures. ***C***, ***D***, Serum samples of Patient 1 at two different time points, from the episode of thymoma and MG (before onset of encephalitis) and from the episode of encephalitis, were analyzed by cell-based ELISA (***C***), and their effects on synaptic GABA$_A$ receptors were investigated (***D***). Average values for GABA$_A$ receptor β3 and LGI1 ELISA from triplicate measurements of the individual serum samples are shown (***C***). Titer of serum antibodies against AchR is shown (bar graph in ***C***; Miyazaki et al., 2012). Synaptic GABA$_A$ receptors were counted as in ***A***. One-way ANOVA with Tukey's *post hoc* analysis; $***p < 0.001$; n.s., not significant. Error bars indicate SEM; $n = 3$ separate cultures.

tection. In support of this, cumulative distribution of the mIPSC amplitude of the patients' serum-treated neurons showed the significant leftward shift (Fig. 6*C*). In contrast, patients' antibodies did not affect AMPA-receptor-mediated mEPSCs (Fig. 6*A*,*D*), which is also consistent with no effects of the patients' antibodies on synaptic AMPA receptor clusters (Fig. 5*A*). Therefore, patients' antibodies specifically reduce the synaptic GABA$_A$ receptor function.

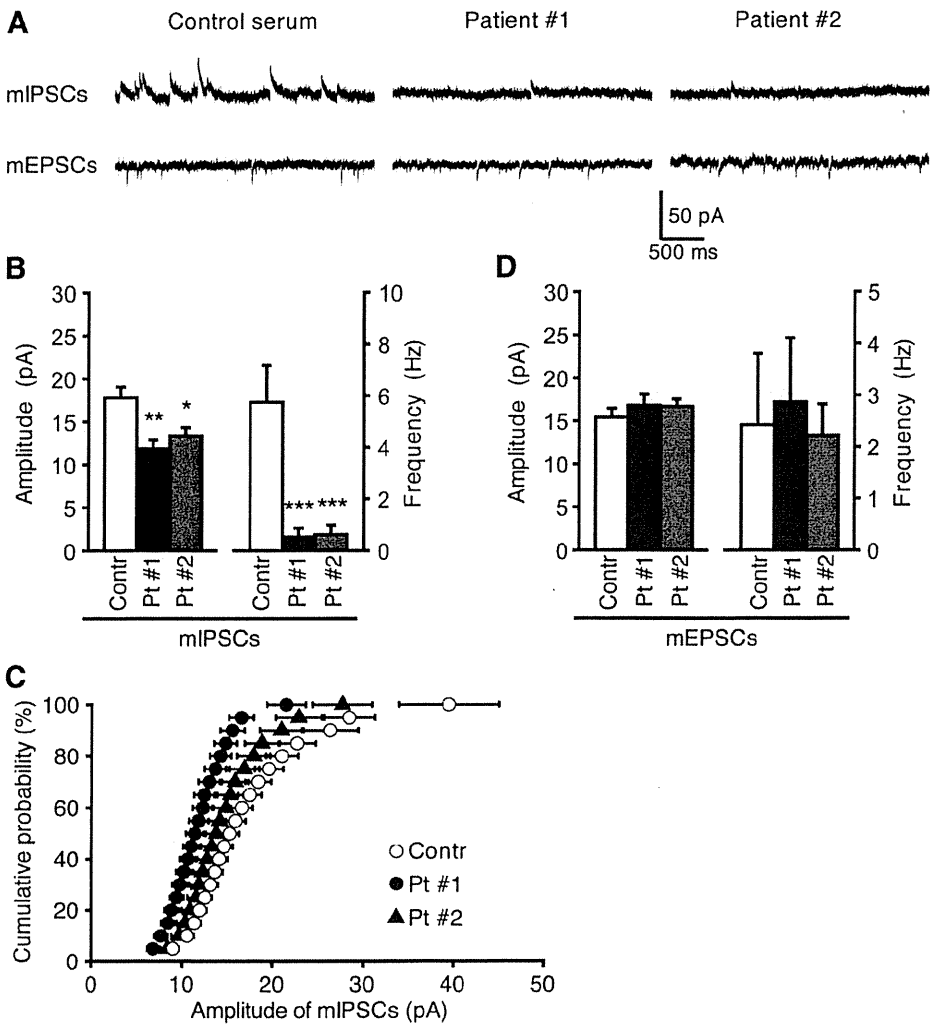

Figure 6. Patients' $GABA_A$ receptor antibodies selectively decrease mIPSCs. *A*, Representative traces of mIPSCs ($V_H = -20$ mV, top) and mEPSCs ($V_H = -80$ mV, bottom) recorded from cultured rat hippocampal neurons, which were incubated with the serum from Patient 1 and Patient 2 or a control individual for 1 d. *B*, *D*, Treatment of neurons with the patient serum significantly decreased the amplitude and frequency in mIPSCs (*B*), but did not affect those in mEPSCs (*D*). Statistical analyses were performed by one-way ANOVA with Scheffe's *post hoc* analysis. $^*p < 0.05$; $^{**}p < 0.01$; $^{***}p < 0.001$ compared with control. *C*, Cumulative distribution of the mIPSC amplitude. Note the significant leftward shift in the amplitude distribution in the patients' serum-treated neurons ($F_{(2, 540)} = 62.9$, $p < 0.001$; two-way ANOVA). Error bars indicate SEM; Control, $n = 9$; Patient 1, $n = 10$; Patient 2, $n = 11$ (*B*, *C*); Control, $n = 9$; Patient 1, $n = 9$; Patient 2, $n = 12$ (*D*). *n* values indicate the number of neurons examined from two separate cultures.

Discussion

Identification of $GABA_A$ receptor autoantibodies in autoimmune encephalitis

GABA is a major inhibitory neurotransmitter and exerts its functions through ionotropic $GABA_A$ receptors and metabotropic $GABA_B$ receptors. $GABA_B$ receptor was recently identified as an autoantigen associated with limbic encephalitis (Lancaster et al., 2010). However, antibodies to the ionotropic $GABA_A$ receptor have not been yet reported in any neuroimmunological disorders. Here, we found the autoantibodies to $GABA_A$ receptors in patients with autoimmune encephalitis and revealed a mode of action of the antibodies. One may wonder why $GABA_A$ receptor autoantibodies have not been found for a long time. One possibility is that the immunoprecipitated band of human IgG (heavy chains) almost completely overlaps with bands of co-isolated $GABA_A$ receptor subunits (all are ~50 kDa) in the SDS-PAGE gel, thereby hindering the detection of $GABA_A$ receptor subunits. Very recently, while this manuscript was under review, a related paper was published reporting the identification of $GABA_A$ receptor autoantibodies in patients with encephalitis showing refractory seizures and/or status epilepticus (Petit-Pedrol et al., 2014). Their history of autoimmunity or cancer seems different from that of our cases. In cases they reported, autoantibodies to $GABA_A$ receptors were sometimes concurrently detected with autoantibodies to GAD65 or $GABA_B$ receptor and were not frequently associated with underlying tumors. In contrast, our cases represent a paraneoplastic subtype of encephalitis with invasive thymoma (Table 1) in which $GABA_A$ receptor autoantibodies coexist with LGI1, CASPR2, or DCC antibodies. It will be worthwhile to test patients presenting with thymoma and encephalitis for $GABA_A$ receptor autoantibodies.

Link between $GABA_A$ receptor autoantibodies and patient symptoms

We found that the $GABA_A$ receptor antibodies of both Patient 1 and Patient 2 targeted the $\beta 3$ subunit of the $GABA_A$ receptor directly. Based on the previous genetic studies showing that mutations in the human $GABA_A$ receptor $\beta 3$ subunit cause genetic

epilepsy syndromes (Macdonald et al., 2010) and that the genetic loss of the β3 subunit causes seizures and learning and memory deficits in mice (DeLorey et al., 1998), it is strongly suggested that the patients' $GABA_A$ receptor antibodies are the direct cause of some CNS disorders such as cognitive impairment and/or seizures often observed in encephalitis. Consistently, both the patients' antibodies similarly showed a selective effect on inhibitory synapses (Figs. 5, 6). In addition, only the serum sample from the episode of encephalitis (Patient 1) had decreased synaptic $GABA_A$ receptor density, whereas the sample of the same patient before the onset of encephalitis had no detectable $GABA_A$ receptor antibodies and no effects on synaptic $GABA_A$ receptor density (Fig. 5*C*,*D*). To further strengthen the link between $GABA_A$ receptor antibodies and patients' symptoms, we considered two additional factors of two patients, "thymoma" and "VGKC-complex antibodies," as follows.

The Patient 1 and Patient 2 both had invasive thymoma (Table 1) (Ohshita et al., 2006; Miyazaki et al., 2012). Because patients with (invasive) thymoma often develop multiple autoantibodies due to disturbed self-tolerance, we included patients with thymoma as controls. Our subjects for the screening contained 19 patients with thymoma, but only two patients had $GABA_A$ receptor antibodies, indicating that not all patients with thymoma develop $GABA_A$ receptor antibodies. For example, the Patient B, with invasive thymoma and myasthenia gravis, had monospecifically DCC antibodies without $GABA_A$ receptor antibodies, whereas Patient C, with invasive thymoma and neuromyotonia, had LGI1 and CASPR2 antibodies without $GABA_A$ receptor antibodies (Fig. 4). Treatment of hippocampal neurons with these patients' serum did not affect synaptic $GABA_A$ receptor clusters (Fig. 5*A* for Patient C; cluster number for Patient B serum, 25.0 ± 4.5/20 μm dendrite and control serum, 25.4 ± 4.2, $p = 0.85$, Student's t test; $n = 11$ neurons).

In addition, we included patients with VGKC-complex antibodies as controls because Patient 1 and Patient 2 both had VGKC-complex antibodies (649 pM for Patient 1; 403 pM for Patient 2; Table 1), which are now attributed to LGI1 and/or CASPR2 antibodies, and previous case reports for these patients showed a correlation between patients' symptoms and the follow-up of VGKC-complex antibodies (Ohshita et al., 2006; Miyazaki et al., 2012). Here, we investigated the serum from Patient C as a control because the patient had VGKC-complex antibodies (809 pM; now revealed as LGI1 and CASPR2 antibodies; Fig. 4) but no $GABA_A$ receptor antibodies. Treatment with this patient serum did not affect the synaptic $GABA_A$ receptor clusters (Fig. 5*A*). In addition, we tested another patient serum with VGKC-complex antibodies (2121 pM) and limbic encephalitis. The patient had high level of monospecific LGI1 antibodies (absorbance = 1.86) without $GABA_A$ receptor antibodies. This serum treatment did not affect the synaptic $GABA_A$ receptor clusters (cluster number for control serum, 27.6 ± 1.2; for the patient serum, 24.6 ± 2.3, $p = 0.39$, Student's t test; $n = 3$ separate cultures). These overall results exclude the possibility that coexisting antibodies other than $GABA_A$ receptor antibodies mediate the effects and support the specific role of $GABA_A$ receptor antibodies in the patients' symptoms.

Two patients with $GABA_A$ receptor antibodies shared some clinical features: cognitive impairment, multifocal abnormal brain MRI signals, and invasive thymoma (Table 1). Importantly, Patient 1 had seizures/status epilepticus, but Patient 2 had no seizure episodes. Given that loss of the β3 subunit in mice causes seizures and learning and memory deficits (DeLorey et al., 1998), it is reasonable to expect that loss of function of the $GABA_A$ receptor mediated by $GABA_A$ receptor β3 antibodies may cause seizures in human patients. However, at present, it seems too early to conclude that $GABA_A$ receptor antibodies should always cause seizures in human patients. It is conceivable that the brain regions where the antibodies act and the amount of the antibodies at different regions can be highly variable between patients. In addition, other factors such as medication and coexisting antibodies may modify the clinical features. In fact, Patient 2 had suffered from postherpetic neuralgia and had been under treatment with carbamazepine, an antiepileptic and anti-nerve-pain drug, for 5 years, including the periods of the initial episode and the relapse of encephalitis (Ohshita et al., 2006) (Table 1). This medication might have prevented the patient's seizure onset. The exact relationship between $GABA_A$ receptor antibodies and specific CNS symptoms will be clarified in the future as the number of cases increases.

Anti-$GABA_A$ receptor encephalitis as a new class of autoimmune encephalitis

The present study indicates that encephalitis associated with $GABA_A$ receptor antibodies shows different clinical features and mechanisms, at least from limbic encephalitis associated with monospecific LGI1 antibodies. Both cases with the $GABA_A$ receptor antibodies showed the similar brain MRI finding, extensive multifocal lesions involving bilateral temporal lobes (Ohshita et al., 2006; Miyazaki et al., 2012). In contrast, limbic encephalitis with LGI1 autoantibodies is featured by the typical MRI finding with the focal lesion of medial temporal lobes (Cash et al., 2011; Lancaster et al., 2011). We previously found that the monospecific serum against LGI1 (ELISA absorbance = 1.86) from a patient with limbic encephalitis significantly reduce synaptic AMPA receptor density of hippocampal neurons (Ohkawa et al., 2013), but the serum did not affect synaptic $GABA_A$ receptor density. Conversely, serum from Patient 1 showed a selective effect on $GABA_A$ receptor function, but did not affect synaptic AMPA receptor density nor mEPSCs regardless of coexisting LGI1 antibodies (absorbance = 0.37; Figs. 5*A*, 6). Unlike NMDA, AMPA, and $GABA_A$ receptor antibodies directly targeting ionotropic receptors to induce the receptor internalization (Lai et al., 2009; Hughes et al., 2010; Fig. 5), LGI1 antibodies need to titrate out endogenous LGI1 to prevent LGI1 from binding to its receptor ADAM22 and then to reduce synaptic AMPA receptors. This indirect mode of action of LGI1 antibodies should require a higher concentration of LGI1 antibodies to be effective. Therefore, the loss of effect of serum from Patient 1 on synaptic AMPA receptors is probably due to the low LGI1 antibody level (Fig. 4*B*) and in turn highlights a predominant role of the $GABA_A$ receptor antibodies in the symptoms experienced by Patient 1. Therefore, it is conceivable that encephalitis with $GABA_A$ receptor antibodies might be distinguished as a new class of autoimmune encephalitis. In addition, we propose that clinical phenotypes of autoimmune anti-$GABA_A$ receptor encephalitis may be further modified by the combination of coexisting autoantibodies such as LGI1, CASPR2, or DCC antibodies, especially if the patient has thymoma. The multiplex ELISA testing to determine the involved autoantibodies will be essential for the accurate diagnosis of a spectrum of autoimmune encephalitis.

In conclusion, we discovered $GABA_A$ receptor autoantibodies associated with autoimmune encephalitis and revealed their pathogenic role, downregulation of the $GABA_A$ receptor function. Given that many agonistic and antagonistic ligands bind to specific sites on the $GABA_A$ receptor, the fine epitope mapping of autoantibodies on the $GABA_A$ receptor β3 subunit may contribute to further understanding the pathogenic mechanism causing

abnormal neuronal excitation in the brain and developing therapeutic interventions.

References

Cash SS, Larvie M, Dalmau J (2011) Case records of the Massachusetts General Hospital. Case 34–2011: A 75-year-old man with memory loss and partial seizures. N Engl J Med 365:1825–1833. CrossRef Medline

Dalmau J, Tüzün E, Wu HY, Masjuan J, Rossi JE, Voloschin A, Baehring JM, Shimazaki H, Koide R, King D, Mason W, Sansing LH, Dichter MA, Rosenfeld MR, Lynch DR (2007) Paraneoplastic anti-N-methyl-D-aspartate receptor encephalitis associated with ovarian teratoma. Ann Neurol 61:25–36. CrossRef Medline

Dalmau J, Gleichman AJ, Hughes EG, Rossi JE, Peng X, Lai M, Dessain SK, Rosenfeld MR, Balice-Gordon R, Lynch DR (2008) Anti-NMDA-receptor encephalitis: case series and analysis of the effects of antibodies. Lancet Neurol 7:1091–1098. CrossRef Medline

DeLorey TM, Handforth A, Anagnostaras SG, Homanics GE, Minassian BA, Asatourian A, Fanselow MS, Delgado-Escueta A, Ellison GD, Olsen RW (1998) Mice lacking the beta3 subunit of the $GABA_A$ receptor have the epilepsy phenotype and many of the behavioral characteristics of Angelman syndrome. J Neurosci 18:8505–8514. Medline

Fang C, Deng L, Keller CA, Fukata M, Fukata Y, Chen G, Lüscher B (2006) GODZ-mediated palmitoylation of $GABA_A$ receptors is required for normal assembly and function of GABAergic inhibitory synapses. J Neurosci 26:12758–12768. CrossRef Medline

Fukata Y, Lovero KL, Iwanaga T, Watanabe A, Yokoi N, Tabuchi K, Shigemoto R, Nicoll RA, Fukata M (2010) Disruption of LGI1-linked synaptic complex causes abnormal synaptic transmission and epilepsy. Proc Natl Acad Sci U S A 107:3799–3804. CrossRef Medline

Fukata Y, Dimitrov A, Boncompain G, Vielemeyer O, Perez F, Fukata M (2013) Local palmitoylation cycles define activity-regulated postsynaptic subdomains. J Cell Biol 202:145–161. CrossRef Medline

Hughes EG, Peng X, Gleichman AJ, Lai M, Zhou L, Tsou R, Parsons TD, Lynch DR, Dalmau J, Balice-Gordon RJ (2010) Cellular and synaptic mechanisms of anti-NMDA receptor encephalitis. J Neurosci 30:5866–5875. CrossRef Medline

Hutchinson M, Waters P, McHugh J, Gorman G, O'Riordan S, Connolly S, Hager H, Yu P, Becker CM, Vincent A (2008) Progressive encephalomyelitis, rigidity, and myoclonus: a novel glycine receptor antibody. Neurology 71:1291–1292. CrossRef Medline

Irani SR, Alexander S, Waters P, Kleopa KA, Pettingill P, Zuliani L, Peles E, Buckley C, Lang B, Vincent A (2010) Antibodies to Kv1 potassium channel-complex proteins leucine-rich, glioma inactivated 1 protein and contactin-associated protein-2 in limbic encephalitis, Morvan's syndrome and acquired neuromyotonia. Brain 133:2734–2748. CrossRef Medline

Jacob TC, Moss SJ, Jurd R (2008) $GABA_A$ receptor trafficking and its role in the dynamic modulation of neuronal inhibition. Nat Rev Neurosci 9:331–343. CrossRef Medline

Lai M, Hughes EG, Peng X, Zhou L, Gleichman AJ, Shu H, Matà S, Kremens D, Vitaliani R, Geschwind MD, Bataller L, Kalb RG, Davis R, Graus F, Lynch DR, Balice-Gordon R, Dalmau J (2009) AMPA receptor antibodies in limbic encephalitis alter synaptic receptor location. Ann Neurol 65:424–434. CrossRef Medline

Lai M, Huijbers MG, Lancaster E, Graus F, Bataller L, Balice-Gordon R, Cowell JK, Dalmau J (2010) Investigation of LGI1 as the antigen in limbic encephalitis previously attributed to potassium channels: a case series. Lancet Neurol 9:776–785. CrossRef Medline

Lancaster E, Dalmau J (2012) Neuronal autoantigens–pathogenesis, associated disorders and antibody testing. Nat Rev Neurol 8:380–390. CrossRef Medline

Lancaster E, Lai M, Peng X, Hughes E, Constantinescu R, Raizer J, Friedman D, Skeen MB, Grisold W, Kimura A, Ohta K, Iizuka T, Guzman M, Graus F, Moss SJ, Balice-Gordon R, Dalmau J (2010) Antibodies to the $GABA_B$ receptor in limbic encephalitis with seizures: case series and characterisation of the antigen. Lancet Neurol 9:67–76. CrossRef Medline

Lancaster E, Martinez-Hernandez E, Dalmau J (2011) Encephalitis and antibodies to synaptic and neuronal cell surface proteins. Neurology 77:179–189. CrossRef Medline

Macdonald RL, Olsen RW (1994) $GABA_A$ receptor channels. Annu Rev Neurosci 17:569–602. CrossRef Medline

Macdonald RL, Kang JQ, Gallagher MJ (2010) Mutations in $GABA_A$ receptor subunits associated with genetic epilepsies. J Physiol 588:1861–1869. CrossRef Medline

McKeon A, Martinez-Hernandez E, Lancaster E, Matsumoto JY, Harvey RJ, McEvoy KM, Pittock SJ, Lennon VA, Dalmau J (2013) Glycine receptor autoimmune spectrum with stiff-man syndrome phenotype. JAMA Neurol 70:44–50. CrossRef Medline

Miyazaki Y, Hirayama M, Watanabe H, Usami N, Yokoi K, Watanabe O, Sobue G (2012) Paraneoplastic encephalitis associated with myasthenia gravis and malignant thymoma. J Clin Neurosci 19:336–338. CrossRef Medline

Moscato EH, Jain A, Peng X, Hughes EG, Dalmau J, Balice-Gordon RJ (2010) Mechanisms underlying autoimmune synaptic encephalitis leading to disorders of memory, behavior and cognition: insights from molecular, cellular and synaptic studies. Eur J Neurosci 32:298–309. CrossRef Medline

Ohkawa T, Fukata Y, Yamasaki M, Miyazaki T, Yokoi N, Takashima H, Watanabe M, Watanabe O, Fukata M (2013) Autoantibodies to epilepsy-related LGI1 in limbic encephalitis neutralize LGI1-ADAM22 interaction and reduce synaptic AMPA receptors. J Neurosci 33:18161–18174. CrossRef Medline

Ohshita T, Kawakami H, Maruyama H, Kohriyama T, Arimura K, Matsumoto M (2006) Voltage-gated potassium channel antibodies associated limbic encephalitis in a patient with invasive thymoma. J Neurol Sci 250:167–169. CrossRef Medline

Petit-Pedrol M, Armangue T, Peng X, Bataller L, Cellucci T, Davis R, McCracken L, Martinez-Hernandez E, Mason WP, Kruer MC, Ritacco DG, Grisold W, Meaney BF, Alcalá C, Sillevis-Smitt P, Titulaer MJ, Balice-Gordon R, Graus F, Dalmau J (2014) Encephalitis with refractory seizures, status epilepticus, and antibodies to the $GABA_A$ receptor: a case series, characterisation of the antigen, and analysis of the eff ects of antibodies. Lancet Neurol 13:276–286. CrossRef Medline

Pirker S, Schwarzer C, Wieselthaler A, Sieghart W, Sperk G (2000) $GABA_A$ receptors: immunocytochemical distribution of 13 subunits in the adult rat brain. Neuroscience 101:815–850. CrossRef Medline

Rudolph U, Knoflach F (2011) Beyond classical benzodiazepines: novel therapeutic potential of $GABA_A$ receptor subtypes. Nat Rev Drug Discov 10:685–697. CrossRef Medline

Satake S, Imoto K (2014) $Ca_v2.1$ channels control multivesicular release by relying on their distance from exocytotic Ca^{2+} sensors at rat cerebellar granule cells. J Neurosci 34:1462–1474. CrossRef Medline

Satake S, Saitow F, Rusakov D, Konishi S (2004) AMPA receptor-mediated presynaptic inhibition at cerebellar GABAergic synapses: a characterization of molecular mechanisms. Eur J Neurosci 19:2464–2474. CrossRef Medline

Sillevis Smitt P, Kinoshita A, De Leeuw B, Moll W, Coesmans M, Jaarsma D, Henzen-Logmans S, Vecht C, De Zeeuw C, Sekiyama N, Nakanishi S, Shigemoto R (2000) Paraneoplastic cerebellar ataxia due to autoantibodies against a glutamate receptor. N Engl J Med 342:21–27. CrossRef Medline

Vincent A, Lang B, Kleopa KA (2006) Autoimmune channelopathies and related neurological disorders. Neuron 52:123–138. CrossRef Medline

Journal of the Peripheral Nervous System 19:311–316 (2014)

RESEARCH REPORT

Neurofilament light mutation causes hereditary motor and sensory neuropathy with pyramidal signs

Akihiro Hashiguchi, Yujiro Higuchi, Miwa Nomura, Tomonori Nakamura, Hitoshi Arata, Junhui Yuan, Akiko Yoshimura, Yuji Okamoto, Eiji Matsuura, and Hiroshi Takashima

Department of Neurology and Geriatrics, Kagoshima University, Graduate School of Medical and Dental Sciences, Kagoshima City, Japan

Abstract To identify novel mutations causing hereditary motor and sensory neuropathy (HMSN) with pyramidal signs, a variant of Charcot-Marie-Tooth disease (CMT), we screened 28 CMT and related genes in four members of an affected Japanese family. Clinical features included weakness of distal lower limb muscles, foot deformity, and mild sensory loss, then late onset of progressive spasticity. Electrophysiological studies revealed widespread neuropathy. Electron microscopic analysis showed abnormal mitochondria and mitochondrial accumulation in the neurons and Schwann cells. Brain magnetic resonance imaging (MRI) revealed an abnormally thin corpus callosum. In all four, microarrays detected a novel heterozygous missense mutation c.1166A>G (p.Y389C) in the gene encoding the light-chain neurofilament protein (NEFL), indicating that *NEFL* mutations can result in a HMSN with pyramidal signs phenotype.

Key words: Charcot-Marie-Tooth disease, gene chip array, hereditary motor and sensory neuropathy with pyramidal signs, light-chain neurofilament protein (NEFL), mitochondrial accumulation

Introduction

Hereditary motor and sensory neuropathy (HMSN) with pyramidal signs includes a genetically and clinically heterogeneous group of neuropathies affecting motor and sensory nerves and the spinal cord. The following three subtypes are identified according to the hereditary pattern: autosomal dominant, autosomal recessive, and X-linked (*Borhoumi et al., 2001; Goto et al., 2003*).

Despite clinical heterogeneity, mutations in only one gene, *mitofusin 2* (*MFN2*), have been linked to HMSN with pyramidal signs *(Zhu et al., 2005)*. In contrast, more than 30 types of hereditary spastic paraplegia (HSP) are caused by mutations in separate genes *(Patel et al., 2002; Irobi et al., 2004; Klebe et al., 2006; Rainier et al., 2008)*. Moreover, these etiologically distinct HMSNs have many overlapping features. Some patients with distal hereditary motor neuropathy 5 (HMN5), resulting from a *BSCL2* mutation, were expressed as a different phenotype with pyramidal signs and slight sensory loss *(Windpassinger et al., 2004; Luigetti et al., 2010)*.

Light-chain neurofilament protein (NEFL) gene encodes the light chain neurofilament protein. Mutations in *NEFL* are associated with demyelinating Charcot-Marie-Tooth disease (CMT) (CMT type 1F), axonal CMT (CMT type 2E), and unspecified CMT *(Mersiyanova et al., 2000; De Jonghe et al., 2001; Georgiou et al., 2002; Yoshihara et al., 2002; Jordanova et al., 2003; Choi et al., 2004; Leung et al., 2006; Miltenberger-Miltenyi et al., 2007; Yum et al., 2009)*. Here we report five generations of a Japanese family with autosomal dominant

Address correspondence to: Dr. Hiroshi Takashima, Department of Neurology and Geriatrics, Kagoshima University, Graduate School of Medical and Dental Sciences, 8-35-1 Sakuragaoka, Kagoshima City, Kagoshima 890-8520, Japan. Tel: +81-99-275-5330; Fax: +81-99-265-7164; E-mail: thiroshi@m3.kufm.kagoshima-u.ac.jp

HMSN with pyramidal signs caused by a novel *NEFL* mutation.

Materials and Methods

We investigated five generations of a Japanese family including 10 individuals with suspected HMSN with pyramidal signs. To confirm the diagnosis and elucidate the underlying genetic cause, four affected members of this family were examined (Fig. 1). The study protocol was reviewed and approved by the Institutional Review Board of Kagoshima University. All family members provided written informed consent.

Standard nerve conduction studies were performed in patient 1 at the age of 57 years and in patient 2 at the age of 65 years. Skin temperature was maintained above 30°C.

A left sural nerve biopsy obtained from patient 2 at the age of 65 years was analyzed for morphometric changes using light and electron microscopes.

Genomic DNA was extracted from the peripheral blood. The custom MyGeneChip® CustomSeq® Resequencing Array (Affymetrix, Inc., Santa Clara, CA, USA) was designed to screen CMT and related diseases such as ataxia with oculomotor apraxia types 1 and 2, spinocerebellar ataxia with axonal neuropathy, and distal hereditary motor neuropathy. We designed 363 primer sets to include the entire coding regions and flanking sequences of the following 28 disease-causing genes: *early growth response 2 (EGR2), peripheral myelin protein 22 (PMP22), myelin protein zero (MPZ), gap junction protein beta 1 (GJB1), periaxin (PRX), lipopolysaccharide-induced TNF-α factor (LITAF), neurofilament light chain polypeptide (NEFL), ganglioside-induced differentiation-associated protein 1 (GDAP1), myotubularin-related protein 2 (MTMR2), SH3 domain and tetratricopeptide repeats 2 (SH3TC2), SET-binding factor 2 (SBF2), N-myc downstream regulated 1 (NDRG1), mitofusin 2 (MFN2), Ras-related GTPase 7 (RAB7), glycyl-tRNA synthetase (GARS), heat shock protein 1 (HSPB1), HSPB8, lamin A/C (LMNA), dynamin 2 (DNM2), tyrosyl-ARS (YARS), alanyl-ARS (AARS), lysyl-ARS (KARS), aprataxin (APTX), senataxin (SETX), tyrosyl-DNA phosphodiesterase 1 (TDP1), desert hedgehog (DHH), gigaxonin 1 (GAN1),* and *K-Cl cotransporter family 3 (KCC3).* In addition, primer sets were designed to include the entire coding regions and flanking sequences of following nine candidate genes: *ankyrin 3 (ANK3), contactin 1 (CNTN1), CNTN2, cysteinyl-ARS (CARS), glutamyl-prolyl-ARS (EPRS), hystidyl-ARS (HARS), methionyl-ARS (MARS), seryl-ARS (SARS),* and *sodium channel, voltage gated, type VIII, alpha subunit (SCN8A).* The details of gene chip analysis have been previously described *(Zhao et al., 2012)*; therefore direct sequencing was performed to confirm the mutations revealed by gene chip analysis.

Results

Patient 1

Patient 1 (IV-6, Fig. 1), a 61-year-old male, developed gradually progressive gait disturbance beginning at age 50. He had a spastic and ataxic gait with mild distal atrophy and diffuse weakness (4/5) in the lower limbs. He had lower limb spasticity, brisk patellar tendon reflexes, and positive Babinski signs. Bilateral *pes cavus* was noted. Light touch and proprioception were decreased in all limbs, whereas vibration was markedly decreased at the ankles. The ankle and upper limb deep tendon reflexes were absent. There was no evidence of extrapyramidal involvement. CMT neuropathy score was 12 *(Murphy et al., 2011).*

Patients 2 and 3

Patients 2 (IV-3, Fig. 1) and 3 (IV-2, Fig. 1) were 66- and 67-year-old brothers of patient 1. They both experienced gait dysfunction and weakness in the lower limbs that started in their mid-50s. Examination revealed *pes cavus*, mild weakness in the lower limbs, absent Achilles tendon reflexes, brisk patellar tendon reflexes, and positive Babinski signs. Vibration was moderately decreased at the ankles. CMT neuropathy score of patient 2 was 9, but patient 3 could not be calculated because of lack of nerve conduction studies.

Patient 4

Patient 4 (III-4, Fig. 1) was the 93-year-old bedridden mother of patients 1, 2, and 3. She suffered from contracture, *pes cavus*, atrophy in the lower limbs, and severe spasticity. She had brisk patellar tendon reflexes and positive Babinski signs but absent Achilles tendon reflexes. CMT neuropathy score could not be calculated.

The thickness of genu (G), middle trunk (MT), and splenium (S) of corpus callosum was measured in the sagittal magnetic resonance imaging (MRI) of patient 1 (T2-weighted) and patient 2 (T1-weighted). In patients 1 and 2, the thickness of G (normal range: 12.6 ± 1.5 mm), MT (normal range: 7.0 ± 0.8 mm), and S (normal range: 12.6 ± 1.6 mm) were 7.1 and 7.9 mm, 3.6 and 3.5, 7.5 and 7.7 mm, respectively *(Okamoto et al., 1990)*. These results revealed thinning of the corpus callosum in both patients (Fig. 2A and 2B). The MRI of the cervical and thoracic spinal cord was normal.

In patient 1, motor nerve conduction velocities (MCVs) of tibial (normal: >41.7 m/s) and peroneal (normal: >41.8 m/s) nerves were 33 and 36 m/s, respectively. Compound muscle action potential (CMAP) of

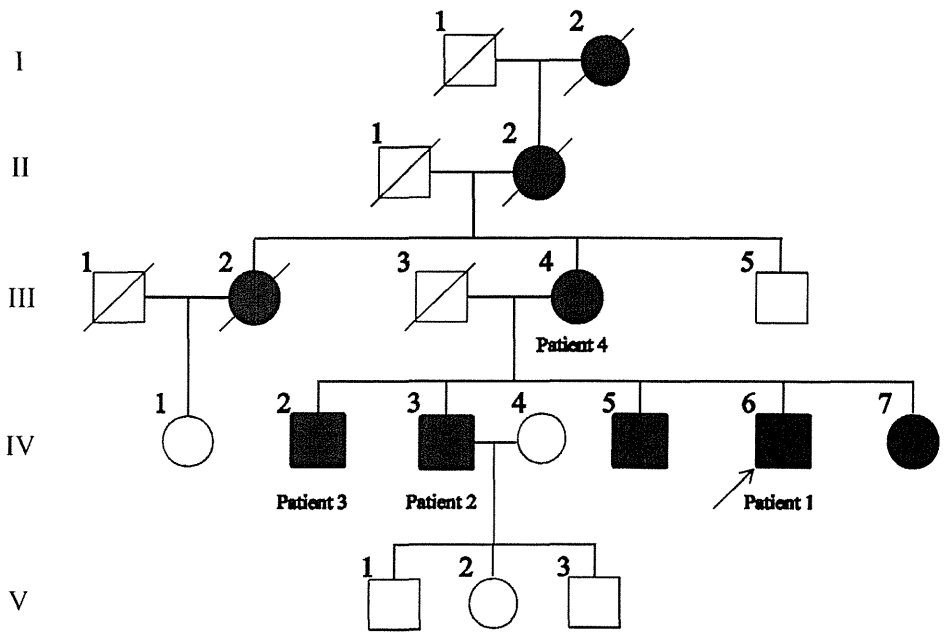

Figure 1. Pedigree of the hereditary motor and sensory neuropathy-V (HMSN-V) family. The arrow indicates the proband. The affected individuals are represented by solid black symbols, and healthy individuals by open symbols.

the tibial nerve (normal: >4.4 mV) was 4.1 mV. The F-wave latencies of the median (normal: <28.2 ms), ulnar (normal: <29.7 ms), and tibial (normal: <51.7 ms) nerves were 33, 30, and 56 ms, respectively. Sensory nerve action potentials (SNAPs) from the median, ulnar, and sural nerves were undetectable. Similarly, in patient 2, MCVs of the tibial and peroneal nerves were 39 and 32 m/s, respectively. CMAPs of the ulnar (normal: > 6.0 mV), tibial, and peroneal (normal: > 2.2 mV) nerves were 3.8, 2.0, and 0.2 mV, respectively. SNAPs from the median, ulnar, and sural nerves were undetectable. The F-wave latency of the tibial nerve was 53 ms. Nerve conduction studies on patients 1 and 2 suggested an axonal type of motor and sensory neuropathy (Table 1). Needle electromyogram was not performed in all patients.

A sural nerve biopsy from patient 2 exhibited slight decrease in large-diameter myelinated fiber densities in all fascicles. Although giant axons and onion bulb formation were not detected, fibers with relatively thin myelin were frequently observed together with occasional small fiber clusters (Fig. 2C). The proportion of myelinated fibers with diameters >6.0 μm was 18%, and the myelinated fiber density was 7,686/mm^2 (>8,000/mm^2). The histogram of myelinated fibers shows unimodal distribution (Fig. 2D). Electron microscopic analysis showed abnormal mitochondria and mitochondrial accumulation in about 10% of neurons and Schwann cells (Fig. 2E and 2F). The accumulation of intermediate filament was not observed.

Using the custom gene chip, we identified a missense heterozygous mutation, c.1166A>G (designated p.Y389C), in exon 2 of *NEFL* in patient 2. Subsequently, the other three affected family members showed the same mutation (Fig. 2G). In healthy family members, no gene testing was done. A sequence homology search was performed to align protein sequences from multiple species using the HomoloGene (http://ncbi.nlm.nih.gov/homologene) system. Tyrosine 389 was conserved among all species analyzed (Fig. 2H). This mutation was neither found in 453 controls with inherited neuropathy nor in the 1,000 Genomes websites listing human genetic variations in 2,500 samples (including 500 East Asian samples). Furthermore, we could computationally predict the effect of the p.Y389C mutation on protein function using the MUpro (http://mupro.proteomics.ics.uci.edu) and PolyPhen-2 (http://genetics.bwh.harvard.edu/pph2/) algorithms. The MUpro score of −0.737 is indicative of a decrease in protein stability (scores <0 indicate a decrease in protein stability) and a PolyPhen-2 score of 1.00 indicates a significant probability of pathogenesis. Using a sequence homology search, we showed that p.Y389 is a completely conserved amino acid residue, suggesting that it may have a potential functional impact on NF-L. In order to exclude diagnosis of HMN5 with pyramidal sign and sensory loss by the *BSCL2* gene mutation, we analyzed that gene by Sanger method resequencing, we did not find any mutation.